universität wien

# MASTERARBEIT / MASTER'S THESIS

Titel der Masterarbeit / Title of the Master's Thesis

## Mesoderm and muscle formation in the quagga mussel, *Dreissena rostriformis* (Deshayes, 1838)


verfasst von / submitted by

Stephan-Matthias Schulreich BSc


angestrebter akademischer Grad / in partial fulfilment of the requirements for the degree of

Master of Science (MSc)

Wien, 2021 / Vienna, 2021

| | |
|---|---|
| Studienkennzahl lt. Studienblatt / degree programme code as it appears on the student record sheet: | UA 066 831 |
| Studienrichtung lt. Studienblatt / degree programme as it appears on the student record sheet: | Masterstudium Zoologie UG2002 |
| Betreut von / Supervisor: | Univ.-Prof. DDr. **Andreas Wanninger** |

# Index

**Abstract**

The mesoderm is a unique feature of bilaterians and gives rise to one of the prominent derivatives, the musculature. Developmental genes with commonly conserved expression during mesoderm and muscle formation are, e.g., *Brachyury* (*Bra*), *even-skipped* (*eve*), *Mox*, and *myosin II heavy chain* (*mhc*). Within the mollusks, the bivalves remain largely unstudied regarding mesodermal gene expression and data on myogenesis likewise remain scarce, given their global distribution and evolutionary significance. Here, myogenesis and developmental expression of *Bra*, *eve*, *Mox*, and *mhc* were investigated in the quagga mussel *Dreissena rostriformis* to contribute to questions concerning the bivalve larval muscular ground pattern and the putative involvement of these genes in mesoderm formation and myogenesis. The data show that all four genes are expressed during mesoderm formation but show additional, individual sites of expression. As such, *Mox* and *mhc* are additionally expressed in early myogenesis. *Eve* expression is present in the shell field, and *Bra* is expressed in the foregut. Comparative analysis suggests that *Mox* has an ancestral role in mesoderm and possibly muscle formation in bilaterians, while *Bra* and *eve* have been conserved in mesoderm development of nephrozoans. The first F-actin-positive domains and a ventro-posterior transitory musculature of unknown function form in the trochophore larva of *D. rostriformis*. In the veliger larva, four pairs of velum retractors, a velum muscle ring, one pair of larval retractors, muscles of the pallial line, two pairs of mantle retractors, one pair of foot retractors and an initially two-partite anterior adductor are present. The posterior adductor was not found in larval stages and might only development shortly before or after metamorphosis. The data presently available suggest that the muscular ground pattern of autobranch bivalve larvae includes at least a velum muscle ring, three or four pairs of velum retractors, one or two pairs of larval retractors, two pairs of foot retractors together with the pedal plexus, possibly two pairs of mantle retractors, the muscles of the pallial line, the anterior (might be paired) and the posterior adductor.

## Introduction

Bilaterian animals have three germ layers, the ectoderm, the endoderm, and the mesoderm. The mesoderm originates during gastrulation and forms a variety of derivatives, including connective tissue, nephridial organ, and musculature (Rieger et al., 2013). Gene expression during mesoderm formation and/or myogenesis have been studied in most bilaterians such as acoelomorphs, deuterostomes including chordates, hemichordates, and echinoderms, as well as in protostomes including ecdysozoans and spiralians (e.g., brachiopods, ectoprocts, phoronids, and annelids; Candia and Wright, 1995; Furlong et al., 2001; Minguillon and Garcia-Fernandez, 2002; Pocock et al., 2004; Lowe et al., 2006; Andrikou et al., 2013; Chiodin et al., 2013; Andrikou and Arnone, 2015; Passamaneck et al., 2015; Erkenbrack, 2016; Kozin et al., 2016; Martín-Durán et al., 2016; Vellutini et al., 2017; Andrikou and Hejnol, 2020). Nevertheless, a large gap of knowledge exists for one of the most morphologically diverse groups, namely the mollusks, for which only few data are currently available (e.g., for the gastropod *Crepidula fornicata* and the bivalve *Saccostrea kegaki*; Kakoi et al., 2008; Perry et al., 2015). Known developmental genes with commonly conserved expression during bilaterian mesoderm formation are, e.g., *Brachyury* (*Bra*), *caudal* (*cdx*), *dachshund* (*dachs*), *even-skipped* (*eve*), *eyes absent* (*eya*), *forkhead A* (*foxA*), *forkhead C* (*foxC*), *forkhead D* (*foxD*), *forkhead F* (*foxF*), *gata4/5/6*, *myocyte enhancer factor-2* (*mef2*), *Mox*, *myosin II heavy chain* (*mhc*), *myoblast determination protein 1* (*myoD*), *neurokinin 1* (*nk1*), *paraxis*, *sine oculis* (*six1/2*), *snail*, *tropomyosin* (*tm*), *twist* (*twi*), and *vasa* (*vas*) (Zhang and Bernstein, 2001; Passamaneck et al., 2015; Martín-Durán et al., 2016; Sebé-Pedrós and Ruiz-Trillo, 2017; Andrikou and Hejnol, 2020). The homeobox gene *Mox* (a homolog of *Meox*, *gax*, or *buttonless*) has been described to have an additional role during myogenesis in some lophotrochozoans and chordates (Passamaneck et al., 2015; Satou and Imai, 2015; Kozin et al., 2016). *Eve* (a homolog of *Evx*, *Xhox3* or *vab-7*) is closely related to *Mox* and acts a pair-rule gene during arthropod

segmentation (Patel et al., 1994; Damen et al., 2000; Copf et al., 2003; Janssen et al., 2011) but was also reported to be involved in mesoderm formation in cephalochordates, vertebrates, and ecdysozoans (Ruiz i Altaba and Melton, 1989; Patel et al., 1992; Ahringer, 1996; Ferrier et al., 2001). In addition, expression of *eve* has been documented during muscle development in some ecdysozoans and in the limb formation in some vertebrates (Ahringer, 1996; Herault et al., 1996; Sordino et al., 1996; Fujioka et al., 2005). Interestingly, in spiralians, *eve* was found to be expressed in the mesoderm of ectoprocts and annelids (Martín-Durán et al., 2016; Kozin et al., 2016; Vellutini et al., 2017). Mesodermal expression of *Bra* was found in the majority of deuterostomes and in some protostomes, including brachiopods, annelids, priapulids and arthropods (Kusch and Reuter, 1999; Peterson et al., 1999; Peter and Davidson, 2011; Martín-Durán et al., 2016; Sebé-Pedrós and Ruiz-Trillo, 2017). In mollusks, no mesodermal expression of *Bra* was found in the gastropod *Haliotis asinina*, whereas in the gastropod *Patella vulgata*, *Bra* is transiently expressed in the 4d cell that gives rise to the future endomesoderm (Koop et al., 2007; Lartillot et al., 2002). In the gastropod *C. fornicata*, *Bra* is involved in mesoderm formation, while in the bivalves *Crassostrea gigas* and *S. kegaki*, the data are somewhat inconclusive as to whether or not *Bra* is expressed during mesoderm development (Kin et al., 2009; Perry et al., 2015; Tan et al., 2017). Myosins comprise a large protein family with a variety of functions, including cytokinesis and myogenesis (Thompson and Langford, 2002; Burgess, 2005). *Mhc* appears to have a conserved role in bilaterian myogenesis and is consistently expressed from the earliest stages of myogenesis onwards (Kobayashi et al., 1998; Zhang and Bernstein, 2001; Renfer et al., 2009; Andrikou et al., 2013).

One of the prominent derivatives of the mesoderm is the musculature. Although larval myoanatomy has been described in a number of taxa, surprisingly few investigations have used state-of-the-art methods such as fluorescence labelling and confocal microscopy to reconstruct bivalve myogenesis in detail. The most detailed studies stem from the shipworm *Lyrodus*

*pedicellatus*, the oyster *C. gigas* and the scallops *Nodipecten nodosus* and *Patinopecten yessoensis* (Wurzinger-Mayer et al., 2014; Audino et al., 2015; Li et al., 2019; Sun et al., 2019). These data showed that bivalve larvae typically exhibit a velum musculature, including velum retractors and a velum muscle ring, as well as larval retractors that degenerate prior to or at metamorphosis. The mantle musculature, including the muscles of the pallial line and the mantle retractors, the adductor system, as well as the foot retractors together with the plexus-like foot musculature, are common features of adult bivalves that develop mostly in the larva and are retained after metamorphosis (Wurzinger-Mayer, 2014; Audino et al., 2015; Cragg, 2016; Li et al., 2019; Sun et al., 2020).

The invasive quagga mussel, *Dreissena rostriformis*, with an indirect lifecycle involving a trochophore larva and a veliger larva, was investigated to gain insights into the expression of "mesodermal" genes as well as myogenesis in bivalve larvae. This study shows whether the putative mesodermal genes *Brachyury*, *even-skipped*, *Mox*, and *myosin II heavy chain* are involved in mesoderm and/or muscle formation of *D. rostriformis* as it has been sown in a variety of bilaterian taxa. On the other hand, novel data about the muscle development of *D. rostriformis* contributes to a reconstruction of the myoanatomical ground pattern of bivalve larvae.

## Material and Methods

### Animal collection, spawning and fixation

Adult quagga mussels were collected from a side branch of the Danube river in Vienna, Austria (Georg-Danzer-Steg, 48°14'45.7"N 16°23'38.4"E), in May 2018. Mussels were kept in a 45 litres aquarium in an incubator at 18°C in Danube water with a weekly water change. Prior to spawning, adult mussels were cleaned with a brush under running tap water. The specimens

were put in a 100 ml beaker with filtered Danube water (FDW) that contained a 0.1% sodium hypochlorite solution (#09951780, DanKlorix, Hamburg, Germany) for five minutes to kill protozoans and rotifers. Afterwards, the mussels were placed in a fresh 100 ml beaker with FDW that contained a $10^{-3}$ M solution of serotonin (#H9523, Sigma-Aldrich, St. Louis, Missouri, USA) for 20 min at room temperature (RT). After that, the animals were placed in fresh individual glass containers with FDW at RT. After spawning, the adult mussels were put in a 200 ml container with FDW at RT. The eggs of each female were mixed with two to three drops of concentrated sperm and transferred to a fresh 200 ml container with FDW at RT. This was followed by three washes in FDW to remove excess sperm. Then the larvae of each female were transferred to a fresh container with 2 litres FDW with aeration and a magnetic stirrer. The cultures were maintained in an incubator at a constant temperature of 18°C. Every other day the water of the larvae was changed with FDW, and then the larvae were fed one to two drops of an *Isochrysis* concentrate (Plankton-Welt, Hamburg, Germany). The oldest larvae were over one month old. For species identification, DNA was extracted from spawning adults using DNeasy Blood & Tissue Kit (#69504, Qiagen, Venlo, Netherlands). Subsequently, PCRs were done by amplifying the extracted DNA with species-specific primers corresponding to mitochondrial cytochrome oxidase 1 (CO1) for *Dreissena rostriformis* (De Ventura et al., 2017).

Developmental stages (gastrula, trochophore larva, early (D-shaped) veliger larva, late veliger larva) of *D. rostriformis* were fixed in 4% paraformaldehyde (PFA) (#158127, Sigma-Aldrich) in phosphate-buffered saline (PBS) (#1058.1, Carl Roth, Karlsruhe, Germany) and placed on ice for 1 h. Before that, crystalline cocaine was added to veliger larvae at a final concentration of 30µg/ml (#609020011, Gatt-Koller, Absam, Austria) to avoid retraction into the shell prior to fixation.

For gene expression analyses, samples were washed twice in 100% methanol and subsequently stored in 100% methanol at -20°C. For immunofluorescence and actin staining, larvae were washed three times in PBS containing 0.1% $N_aN_3$ (#71289, Sigma-Aldrich) and stored at 4 °C.

**Bioinformatic analysis**

Most orthologs of the genes of interest (*myosin II heavy chain*, *Mox*, *even-skipped* and *Brachyury*) and corresponding outgroups of the genes were retrieved from the NCBI database (www.ncbi.nlm.nih.gov) (Table 1-3) for comparison with *Dreissena rostriformis* sequences (Calcino et al., 2019) using BLASTp, Version 2.8.1+ (Altschul et al., 1990). Additionally, a few orthologs were downloaded from the Ensembl Metazoa database (Table 1 and 3) in order to generate the related outgroups of the genes of interest as well as for the generation of some orthologs of *Dreissena rostriformis* in the corresponding outgroups. Therefore, the hmm file of the myosin-head domain and the T-box domain from Pfam, Version 32.0 (Stockholm, Germany, www.pfam.xfam.org) were retrieved. The genome (protein database) of a bivalve *Crassostrea gigas* and the cnidarian *Nematostella vectensis* were downloaded (Howe et al., 2020, Hinxton, United Kingdom, https://metazoa.ensembl.org/index.html) and were used for the hmmscan. In addition, some orthologs of the genes of interest of *Acanthochitona crinita* were added from the transcriptome (De Oliveira et al., 2016; https://zoology.univie.ac.at/research/open-data/). For the *myosin II heavy chain* phylogeny, metazoan-specific *myosin* families were included. (Thompson and Langford, 2002). All selected *myosin* families contain a myosin-head domain with *myosin I* being the predicted earliest sequence offshoot that was thus used as outgroup (Foth et al., 2006). For the *even-skipped* and *Mox* phylogeny, several *Hox* genes families were used as outgroup, all of which contain a homeodomain (Ryan et al., 2007; Minguillón and Garcia-Fernàndez, 2003). For the *Brachyury* phylogeny, all metazoan-specific *T-box* families were included. *Brachyury* is an

ancient group of *T-box* families and was used as an outgroup (Sebé-Pedrós et al., 2013; Sebé-Pedrós and Ruiz-Trillo, 2017). The specific amino acid Lysine (K) in the DNA-binding domain within the T-box domain is characteristic for *Brachyury* (Conlon et al., 2001; Sebé-Pedrós et al., 2013).

Multiple alignment was done using MAFFT, Version 7.427 (Katoh et al., 2002). Subsequently, the data were trimmed with BMGE, Version 1.12 (Criscuolo and Gribaldo, 2010). Appropriate substitution models for amino acid were calculated using ProtTest, Version 2.1 (Abascal et al., 2005). These were LG (Le and Gascuel, 2008) for *Brachyury* and *myosin II heavy chain* and JTT (Jones et al., 1992) for e*ven-skipped* and *Mox*. The phylogenetic (maximum likelihood) trees were computed using PHYML, Version 20120412 (Guindon and Gascuel, 2003) with a bootstrap value of 100. The sequence alignments were visualised with AliView, Version 1.0.0.0 (Larsson, 2014). Jalview, Version 2.11.0 (Waterhouse et al., 2009) was used to change the font and colour of the alignment. Gimp, Version 2.10.14 (www.gimp.org/downloads/) was used for a better resolution (1000) and to smoothen the alignment. Visualisation of phylogenetic trees was done using FigTree, Version 1.4.4 (www.tree.bio.ed.ac.uk/software/figtree/). All trees were re-rooted with the above-mentioned ancient or sister gene family. Specific primers of investigated genes for *in situ* hybridization were designed (www.promega.com, Table 4) and synthesised by Microsynth Austria GmbH (Vienna, Austria). The primers were diluted to yield a working concentration of 10 µM and stored at -20°C. The nucleotide sequence length with corresponding forward and reverse are listed in Table 4. Relative gene expression values were produced for all four genes of interest using stage-specific transcriptomes of *D. rostriformis* (Calcino et al., 2019).

**RNA extraction and probe synthesis**

RNA extraction was done following the manufacturer's instructions, and modifications are mentioned in the following where they occurred. All PCRs (cDNA-, plasmid-, colony- PCR) were done using Go Taq Flexi DNA Polymerase (0,025u/µl, #M780B, Promega, Madison Wisconsin, USA), 1x Go Taq Flexi Buffer (#M890A, Promega), PCR nucleotide mix (0,8mM, #C1145, Promega), 1,25 mM $MgCl_2$ (#A351H, Promega), and nuclease-free water (#R0581, Thermo Fisher Scientific, Waltham, Massachusetts, USA).

Different developmental stages (1, 2, 4, 6, 8, 12, 15, 18, 21, 24, 28, 48, 70 hours post fertilization; hpf) were transferred in RNAlater (#76106, Qiagen, Venlo, Netherlands) and stored at 4°C. The total RNA extraction of pooled stages was created using the RNeasy Mini Kit (#74104, Qiagen) with the QIAshredder homogenizer (# 79654, Qiagen). The RNA extraction samples were diluted by 1:10 with DEPC- (diethylpyrocarbonate-) treated water and quantified by spectrophotometer (Nanodrop 2000c, Thermo Fisher Scientific). Purified RNA samples were stored at -20°C. The total RNA was denatured for 15 min at 65°C and placed on ice. Subsequently, the first-strand cDNA synthesis was done using 1$^{st}$ Strand cDNA Synthesis Kit for RT-PCR (#11 483 188 001, Roche, Basel, Switzerland) using Oligo-p$(dt)_{15}$ primers. The resulting cDNA was diluted 1:5, stored at -20°C and used as a cDNA template. Several PCRs were done with cDNA and the corresponding primers to amplify *Brachyury*, *even-skipped,* and *myosin II heavy chain* (Table 4). *Mox* was amplified with the mix described above but with undiluted cDNA. The annealing temperatures for the PCR depended on the individual genes: 55°C for *even-skipped* and *myosin II heavy chain* and 53°C for *Brachyury* and *Mox*, each with 35 cycles. The PCR products were checked using gel electrophoresis with a 1% agarose gel (#2267.4, Carl Roth, Karlsruhe, Germany) in TAE buffer (#CL86.1, Carl Roth). The corresponding band with the respective nucleotide sequence length of the genes of interest were excised, and the DNA was extracted using a QIAquick Gel Extraction Kit (#28706, Qiagen).

The extracted DNA (insert) was stored at -20°C. Ligation of the insert into the plasmid and the transformation of the plasmid into *E. coli* JM109 Competent Cells on an LB-agar (0,035g/ml, #965.1, Carl Roth) plate with 0.1% ampicillin (#A9518, Sigma-Aldrich) were done using pGEM-T Easy Vector System II product (#A1380, Promega). Ligation products were stored for one or two days at 4°C, and the transformations were stored in an incubator overnight at 37°C. White colonies (different clones of the gene) on the agar plate which contained the plasmid were selected and were picked with a toothpick and dipped into a PCR tube with water for a colony PCR. The toothpick was put in a glass tube with 5 ml LB medium (#X964.1, Carl Roth) containing ampicillin (100µg/ml, #A9518, Sigma-Aldrich) and the glass tube was placed on the shaker (180RPM) overnight at 37°C for the growth of the transformed colony. The colony PCR was done using the reverse (CAGGAAACAGCTATGAC) and forward (TGTAAAACGACGGCCAG) M13 primers (10µM, Microsynth, Balgach, Switzerland) (annealing temperature of 55°C, 45 s, 30 cycles), followed by gel electrophoresis. Visible bands were compared with the gel electrophoresis from the cDNA PCR of the respective genes, and useful clones were selected for the miniprep. Plasmid DNA purification was done using QIAprep Spin Miniprep Kit (#27106, Qiagen). Concentrations were checked with the spectrophotometer (Nanodrop 2000c, Thermo Fisher Scientific) and sequenced (Microsynth, Vienna, Austria). The inserts of plasmids were multiplied using a plasmid PCR with the above-mentioned forward and reverse M13 primers (annealing temperature of 55°C, 45 s, 30 cycles). Afterwards, the PCR products were controlled by gel electrophoresis and stored at 4°C. The in vitro transcription and riboprobe (antisense and sense probes) production was done mixing Rnase-free water (#R0581, Thermo Fisher Scientific), 1x transcription buffer (#11465384001, Roche), 10µM dithiothreitol (DTT, #D9779, Sigma-Aldrich), 1x DIG RNA Labelling Mix (#11277073910, Roche), 0,1u Protector RNase Inhibitor (#03335402001, Roche), 50u SP6 RNA polymerase (#10810274001, Roche) or 50u T7 RNA polymerase (#10881767001, Roche), and PCR product in a PCR tube. The PCR mixes were placed into a thermocycler

(37°C, lid 60°C) for 2 h. Afterwards, 1 µl Dnase I recombinant, Rnase-free (#04716728001, Roche) was added to PCR mixes to remove template DNA. The PCR mixes were placed again into a thermocycler at 37°C for 15 min. The purification of DIG-Probes was done using ProbeQuant$^{TM}$ G-50 Micro Columns (#GE28-9034-08, GE Healthcare). Subsequently, 5µl 4M LiCl (#L7026, Sigma-Aldrich) and 120µl 100% EtOH (#20821, VWR Chemicals) were added to the riboprobes and incubated overnight at -20°C. Next, the riboprobes were placed into a centrifuge (14 000 rpm) for 15 min at 4°C and washed twice with 70% EtOH. Afterwards, the riboprobes were dried for 15 min at RT and dissolved in 20µl Rnase-free water (#R0581, Thermo Fisher Scientific). All RNA probes were quantified using a spectrophotometer and controlled by gel electrophoresis. The RNA riboprobes were stored at -80°C until further use.

**Whole mount *in situ* hybridization (WMISH)**

For the WMISH experiments, the first candidate of *Dreissena rostriformis myosin II heavy chain* (*Dro-mhc_c1*) was used, as it was shown to be the most similar sequence compared with other species (Figure 1A). The single *Dreissena rostriformis even-skipped* (*Dro-eve*) and the single *Dreissena rostriformis Brachyury* (*Dro-Bra*), as well as the second candidate of *Dreissena rostriformis Mox* (*Dro-Mox_c2*), which was shown to be the more highly expressed of the two orthologs, were selected for WMISH experiments (Table 5).

*Dreissena rostriformis* samples were stepwise transferred from 100% methanol into PBS (#1058.1, Carl Roth). All samples were decalcified for 1 h in PPE (4% PFA (#158127, Sigma-Aldrich), PBS, 50mM pH8 EGTA (#E3889, Sigma-Aldrich)) and washed three times for five min each in PBT (1xPBS, 0.1% Tween 20; #9127.1, Carl Roth). Subsequently, the larvae were incubated in 30µg/ml proteinase-K (#03115879001, Roche) solution for 10 min at 37°C. After that, the specimens were washed three times for five min each in PBT, followed by post-fixation

in 4% PFA for 45 min and washed again three times for five min each in PBT. Subsequently, the larvae were stepped into 100% hybridization buffer (50% formamide (#47671, Sigma-Aldrich), 5x SSC (#10541, Carl Roth), 50-100 µg/ml heparin (#H3149, Sigma-Aldrich), 5mM EDTA pH8 (#20-158, Sigma-Aldrich), 1x Denhardt´s (#D2532, Sigma-Aldrich), 100µg/ml yeast tRNA (#R6750, Sigma-Aldrich), 0.1% Tween 20 (#9127.1, Carl Roth), 5% dextransulfat (#D8906, Sigma-Aldrich)). After that, the samples were pre-hybridized in a water bath overnight, for which the temperature was specific for each gene (58,5°C for *myosin II heavy chain* and 55°C for *Mox*, *even-skipped* and *Brachyury*). Antisense probes and sense probes for negative controls were mixed with the hybridization buffer (2ng/µl) and put into a heat plate for 10 min at 85°C. The riboprobes were added to the specimens for the hybridization and incubated for 48-60 h in the water bath. Afterwards, the samples were washed three times for 20 min each in 4x Wash (50% formamide (#47671, Sigma-Aldrich), 4x SSC (#10541, Carl Roth), 0.1% Tween 20 (#9127.1, Carl Roth)), followed by two washes for 20 min each in 2x Wash (with 2x SSC) and then washed twice for 15 min each in 1x Wash (with 1 x SSC). Next, all specimens were washed three times for 15 min each in 1x SSC (#10541, Carl Roth) containing 0.1% Tween 20 (#9127.1, Carl Roth) at RT. Subsequently, all samples were stepped into 0,1 M MAB (100mM maleic acid (#K304.1, Roth), 150mM NaCl (#6781.3, Carl Roth), 0.1 % Tween 20 (#9127.1, Carl Roth)) at RT. After that, the larvae were incubated for 3 h in a 2% block solution (#11096176001, Roche) in 0,1 M MAB at RT. The specimens were placed in a 2% block solution in 0,1 M MAB with Anti-Digoxigenin-AP Fab fragments (#11093274910, Roche) in a solution of 1:5000 overnight at 4°C. Next, the samples were washed three times for 20 min each, followed by three times for 10 min each in PBT. The larvae were washed twice for five min each in AP buffer (1x alkaline phosphatase, 1M NaCl (#6781.3, Carl Roth), 200mM Tris pH9 (#4855.1, Carl Roth), 0.1% Tween 20 (#9127.1, Carl Roth)) prior to staining. For highly expressed genes (e.g., *myosin II heavy chain*), the specimens were stained with a colour reaction buffer (1x AP buffer, 0.005% NBT (Nitroblue tetrazolium

chloride, #11383213001, Roche), 0.00375% BCIP (5-Bromo-cloro-3-indolyl-phosphate, 4-toluidine salt (#11383221001, Roche)), and colour was developed at 37°C for 2-3 h. The samples of lowly expressed genes were stained with the same above-mentioned colour reaction buffer with 7.5% polyvinyl alcohol (PVA) (#P1763, Sigma-Aldrich), and dye was developed at 37°C for 4-13.5 h. In order to stop the reaction, the larvae were washed twice for 5 min each in PBT, and then the specimens were post-fixed in 4% PFA for 1 h at 4°C. Subsequently, the specimens were washed three times for 5 min each in PBT, followed by three washing steps in PBS for 10 min each. All washing steps were done on a shaker with 130 RPM at RT. The larvae were stored at 4°C, and the PBS was changed once a week. For the subsequent analyses, the samples were mounted on glass slides in 100% glycerol (#G5516, Sigma-Aldrich) and visualised and documented with an Olympus BX53 light microscope with an Olympus DP73 camera and the software cellSens Standard, Version 1.11 (Olympus Corporation, Shinjuku, Tokyo, Japan). Schematic drawings were created with Inkscape, Version 0.92.4 (www.inkscape.org/de/release/inkscape-0.92.4/).

**Fluorescence staining**

*Dreissena rostriformis* samples were washed three times for 10 min each in PBS, followed by decalcification for 1 h in 50 mM EGTA (#E3889, Sigma-Aldrich) in PBT and two washes for 10 min each in PBT at RT. Unspecific binding sites were blocked for 1 h in PBT with 3% normal swine Serum (#014-000-121, Jackson ImmunoResearch, West Grove, Pennsylvania, USA). Subsequently, samples were incubated in the primary antibodies (dilution 1:900, Anti-acetylated α-Tubulin, #T6793, Sigma-Aldrich) in the block solution overnight at RT. All specimens were washed five times for 15 min each in PBT and incubated in secondary antibodies (dilution 1:900, Goat anti-mouse, Alexa Fluor 633, #A21050, Invitrogen) with DAPI (dilution 1:400, 4',6-diamidino-2-phenylindole, #D1306, Invitrogen, Carlsbad, California,

USA) added to visualize cell nuclei and Alexa Fluor 488 phalloidin (dilution 1:40, #A12379, Invitrogen) for actin labeling in PBT for 24 h at 4°C in the dark. All samples were washed five times for 15 min each in PBT, followed by two washing steps in PBS for 10 min each. Stained specimens were mounted on glass slides with Fluoromount-G (#0100-01, SouthernBiotech, Birmingham, AL, USA). The samples were stored at 4°C in the dark for a few days prior to the analyses. Samples were analysed with a Leica SP5 II confocal laser scanning microscope with the software LAS AF, Version 2.6.3.8173 (both Leica Microsystems, Wetzlar, Germany). ImageJ2 (Rasband, W.S., ImageJ, U. S. National Institutes of Health, Bethesda, Maryland, USA, https://imagej.nih.gov/ij/, 1997-2018) and Imaris x64, Version 7.3.1 (Bitplane, Zurich, Switzerland) were used to analyse the image stacks and Inkscape, Version 0.92.4 was used to create the schematic drawings.

## Results

### Phylogenetic analyses of genes of interest

All annotated genes of interest are summarized in Table 6. For the *myosin II heavy chain* family, four candidates (*Dro-mhc_c1*, *c2*, *c3*, *c4*) were found, which contain a specific glycine insertion (G) at position 534 (Figure 1). The first three candidates (*Dro-mhc_c1-c3*) include a complete myosin N, myosin head and myosin tail 1 domain. The fourth candidate (*Dro-mhc_c4*) contains a fragmented myosin head domain (Table 6). Nine further candidates (twice *myosin I*, *myosin III*, *myosin V*, *myosin VI*, *myosin VII*, *myosin IX*, *myosin XV* and *myosin XVIII*) with partially fragmented myosin head domains were found in *D. rostriformis* and nest within the corresponding *myosin* family (Figure 1A and Table 6).

A phylogenetic tree was constructed for the homeobox domain-containing *even-skipped* and *Mox* genes (Figure 2). A single *D. rostriformis even-skipped* (*Dro-eve*) ortholog was identified,

which includes a tyrosine (Y) at position 48 at the beginning of the homeobox domain (Figure 2A, B). Two *D. rostriformis Mox* (*Dro-Mox_c1* and *Dro-Mox_c2*) orthologs were found, which contain a glutamic acid (E) insertion at position 48 at the beginning of the homeobox domain (Figure 2A, C). The third *Mox* candidate nests within the *Hox4* family (Figure 2A).

A single *D. rostriformis Brachyury* (*Dro-Bra*) ortholog nests within the *Brachyury* family, which includes a specific Lysine (K) at position 121 (Figure 3). Six further candidates (*Eomes*, *Tbx2*, *Tbx3*, *Tbx15*, twice *Tbx20*) with a T-box domain were found in *D. rostriformis* and nest within the corresponding family (Figure 3 and Table 6).

**Orientation and characteristics of developmental stages**

At 18°C, a free-swimming, ciliated gastrula has formed after 18 hours post fertilisation (hpf). The developing shell field is characterised by a deep invagination on the dorsal side that is surrounded by large ectodermal cells, while the blastopore marks the ventral side (Figure 4A). At about 24 hpf, the early trochophore larva has developed (Figure 4B). Evagination of the shell field commences and is completed by approximately 30 hpf. A ciliated, two-rowed prototroch is distinct, together with an apical tuft and a posterior telotroch (Figure 4C, D). Between 30 and 40 hpf, an early (D-shaped) veliger larva has developed (Figure 4E-G). The veliger larva is characterised by two lateral valves that form the embryonic shell (protoconch I: often referred to prodissoconch in bivalves; see Wanninger and Wollesen 2015) and by a ciliated velum that has developed from the prototroch. In addition, *Dreissena* veliger larvae also exhibit a pre-anal tuft on the ventral side and a telotroch on the ventro-posterior side, as well as a functional digestive tract (Figures 4E-I). After 4-5 days, the D-shape of the veliger larva changes and the umbo begins to form (Figures 4H, I). The oldest veliger larvae were over one month old, but no settlement or metamorphosis was observed.

**Developmental expression of *Brachyury* and *even-skipped***

The relative values of the quantitative analysis of the genes of interest are summarized in Table 5. *Dro-Bra* shows high relative expression during the early stages (< 18 hpf), with a considerable decrease in the gastrula stage (18 – 23 hpf). Relative expression values remain low in the trochophore (23 – 30 hpf) and veliger stage (> 30 hpf) (Figure 5A and Table 5). The two earliest *Dro-Bra* expression domains are in the developing mesoderm at the ventral region of the gastrula (18 hpf) (Figures 4A and 6 A, B). In the trochophore larva (30 hpf), *Dro-Bra* is expressed in the endoderm along the region corresponding to the invagination of the developing digestive tract, on either side (Figures 4D and 6C, E). In addition, expression of *Dro-Bra* is present in the ventro-posterior mesoderm and is located posteriorly to the developing digestive tract in the region of the future hindgut (Figures 4D and 6C, D). No expression of *Dro-Bra* was found in the veliger larva.

The quantitative analysis of *Dro-eve* transcripts shows a high relative expression in early stages (< 18 hpf), with a considerable decrease in the gastrula stage (18 – 23 hpf) and a slight decrease in the trochophore stage (23 – 30 hpf). Relative expression values remain low in the veliger stage (>30 hpf) (Figure 5A and Table 5). The earliest expression domains of *Dro-eve* are present in the gastrula stage (18 hpf). One of them is expressed ectodermally in the shell field on the dorsal side (Figure 4A and 7A, C). Two expression domains are situated in the developing mesoderm at the ventral region (Figures 4A and 7A, B). The mesodermal expression domains lie in the region of the expression of *Dro-Bra* (Figures 4A and 6A, B). In the trochophore larva (30 hpf), two *Dro-eve* expression domains are found, namely in the ectoderm at the median region of the shell field on the dorsal side as well as in the ventro-posterior mesoderm (Figures 4A and 7D, E). The mesodermal expression of *Dro-eve* is located posteriorly to the developing digestive tract and lies adjacent to the expression of *Dro-Bra,* with the former extending further

laterally (Figures 6C, D and 7D, E). No expression domains of *Dro-eve* were found in the veliger larva.

**Developmental expression of *myosin II heavy chain***

The quantitative analysis of all *Dro-mhc* candidates shows a low relative expression during early stages (< 18 hpf), with a slight increase in the gastrula stage (18 – 23 hpf), followed by further increase in the trochophore stage (23 – 30 hpf) and, more dramatically, in the veliger stage (> 30 hpf) with two significant peaks (36 hpf and between 60 – 72 hpf) (Figure 5B and Table 5). The two earliest *Dro-mhc_c1* expression domains are found in the anterior mesoderm of the early trochophore larva (24 hpf). They are spot-like expression domains and are situated in the anterior region between the developing digestive tract and the shell field (Figures 4B and 8A, B). These spot-like expression domains are in the region of the first F-actin positive cells, which appear at around 30 hpf (Figures 4C and 8C, D). In the trochophore larva (30 hpf), four expression domains of *Dro-mhc_c1* are present in the dorsal mesoderm. Two of them are stripe-like expression domains, they are elongated along the anterior-posterior axis (Figures 4C and 9E, G) and are at the site of the developing dorsal velum retractors and the larval retractors (Figures 4D and 9I, K). The other two are spot-like expression domains, they are located in the dorso-anterior region (Figures 4C and 9E, G, H) and are at the site of the anlagen of the anterior adductors (Figures 4D and 9I, K, L). Additionally, four expression domains are found in the ventral mesoderm. They are adjacent to and posterior of the developing digestive tract, on either side (Figures 4C and 9E, F, H) and are in the region of the ventro-posterior musculature (Figures 4D and 9I, J, L) and at the site of *Dro-Mox_c2* (Figures 4C and 9A, B, D). However, the ventral expression domains of *Dro-mhc_c1* are slightly larger than those of *Dro-Mox_c2* (Figures 4C and 9B, F).

In the D-shaped veliger larva (70 hpf), three expression domains of *Dro-mhc_c1* are present. Two of them are lateral on both sides at the median region of the larva (Figures 4E and 10A, E) and are at the site of the velum retractors and larval retractors (Figures 4F, G and 10B-D). The third expression domain is in the dorsal region between the shell plates (Figures 4E and 10A, E) and are at the site of the developing anterior adductors (Figures 4I and 10B-D).

## ***Mox* expression**

The quantitative analysis of *Dro-Mox_c2* shows a very weak relative expression until the gastrula stage (13 – 23 hpf, see Table 5), followed by a slight increase and subsequent decrease in the trochophore stage (23 – 30 hpf). In the early veliger stage, a short increase with a subsequent decrease (30 – 48 hpf) is followed by very low relative expression values (> 48 hpf) (Figure 5A and Table 5). The earliest *Dro-Mox_c2* expression domains are found in the mesoderm in the ventral region of the trochophore larva (30 hpf). Expression of *Dro-Mox_c2* is adjacent to and posterior of the developing digestive tract, on either side (Figures 4C and 9A, B, D). These expression domains are in the region of the ventro-posterior musculature (Figures 4D and 9I, J, L) and at the site of the ventral expression of *Dro-mhc_c1* (Figures 4C and 9E, F, H). No *Dro-Mox_c2* expression was found in the veliger larva.

## **Myogenesis**

The earliest F-actin-positive domains are in the dorso-median mesoderm in the *D. rostriformis* trochophore larva (30 hpf). They are paired and are situated below the median region of the shell field (Figures 4C and 8C, D). Shortly later, the first pair of myofilaments emerges, which consists of the developing dorsal velum retractors and the developing ventral larval retractors

and lie below the shell field. The developing dorsal velum retractors project into the anterior region. In contrast, the developing ventral larval retractors extend into the posterior region with slightly ventral direction (Figures 4D and 9I, K). Additionally, in the trochophore larva, the first pair of F-actin-positive domains of the anterior adductors forms in the dorso-anterior mesoderm. These domains lie below the shell field and above the developing dorsal velum retractors (Figures 4D and 9I, K, L). In addition, a pair of transient ventro-posterior musculature emerges in the ventral region and lies posterior to the developing digestive tract (Figures 4D and 9I, J, L).

The first distinct muscle bundles develop in the early (D-shaped) veliger larva (40 hpf). The mantle (pallial) musculature is formed around the edges of the mantle (Figures 4F and 10B). Two fine interconnections of the anterior adductors are visible and attach dorsally to the embryonic shell (Figures 4F, I and 10B, C). A pair of ventral larval retractors attaches to the embryonic shell near the hinge and extends ventrally into the region of the hindgut (Figures 4F and 10B). The velum musculature consists of the newly formed velum muscle ring that underlies the velum (Figures 4F and 10B). In addition, a pair of dorsal velum retractors inserts posteriorly at the embryonic shell near the hinge and at the dorsal part of the velum (Figures 4F and 10B, D). The second pair of velum retractors, the ventral velum retractors, develops between the dorsal velum retractors and the ventral larval retractors and attaches in the median region of the velum and posteriorly at the embryonic shell near the hinge (Figures 4F and 10B, D). The third pair of velum retractors, the median velum retractors, emerges shortly later in the D-shape veliger larva. The attachment is posterior to the embryonic shell near the hinge and at the velum between the dorsal velum retractors and the ventral velum retractors (Figures 4G and 10D). A median branch of the median velum retractors runs towards the ventral part in the region of the hindgut. This branch shows a connection to the median velum retractor (Figures 4G and 10C, H). In the late veliger larva (102 hpf), the fourth pair of velum retractors (accessory

velum retractors), two pairs of mantle retractors, and one pair of foot retractors appear (Figures 4H and 10G). The accessory velum retractors are located between the anterior adductors and the dorsal velum retractors and attach to the most dorsal region of the velum. Two pairs of mantle retractors are situated between the dorsal and the ventral velum retractors, respectively, and both connect to the mantle. The foot retractor emerges as a branch of the dorsal velum retractor and extends into the region of the developing foot (Figures 4H and 10G). In the late veliger larva, the anterior adductors increase in size (Figures 4H, I and 10 F-I). Shortly later, the foot retractors get interconnected and form a U-shape (Figures 4I and 10H, I).

## Discussion

### Comparative *Brachyury* expression in Bilateria

In *Dreissena rostriformis*, *Bra* is expressed in the developing mesoderm in the gastrula stage and in the trochophore larva, with additional expression in the developing foregut in the latter. A very similar *Bra* expression pattern is found in the putative mesoderm in the ventral region in the gastrula of the Pacific oyster *Crassostrea gigas* (Tan et al., 2017). In the spiny oyster *Saccostrea kegaki*, first *Bra* expression is in the vegetal region of the 16-cell stage. After that, *Bra* is also expressed in the putative mesoderm in the ventral region, similar to *C. gigas* and *D. rostriformis*. In *S. kegaki*, *Bra* is additionally expressed in the ectoderm along the ventral midline and near the blastopore. After the evagination of the shell field, *Bra* is restricted to the presumptive anus region, similar to *D. rostriformis*. However, in contrast to *D. rostriformis*, no *Bra* expression was found in the foregut of *S. kegaki* (Kin et al., 2009). In most gastropods, *Bra* expression pattern is similar to that of bivalves, where *Bra* is expressed in the mesoderm, digestive tract, as well as ectodermally near the blastopore, and along the ventral midline (Figure 11; Lartillot et al., 2002; Perry et al., 2015). Since the latter expression domain is only

present in most mollusks, it seems to be an apomorphy of Molluska, while the other expression domains also occur in other taxa (Figure 11).

*Bra* expression has been described near and/or around the blastopore as well as in the digestive tract in a vast number of metazoans, except in ctenophore *Mnemiopsis leidyi*, where *Bra* is expressed only around the blastopore (Figure 11; Peter and Davidson, 2011; Green and Akam, 2014; Hejnol and Martín-Durán, 2015; Martín-Durán et al., 2016; Sebé-Pedrós and Ruiz-Trillo, 2017). This indicates that *Bra* appears to have a conserved role in blastopore and digestive tract formation among bilaterian animals (Figure 11). Mesodermal expression of *Bra* has been reported in most nephrozoan taxa, while in a few spiralians, e.g., ectoprocts, phoronids and chaetognaths, as well as in a subclade of chordates, the tunicates, *Bra* was not found to be expressed in the mesoderm (Figure 11; Terazawa and Satoh, 1997; Kusch and Reuter, 1999; Peterson et al., 1999; Nishino et al., 2001; Takada et al., 2002; Peter and Davidson, 2011; Martín-Durán et al., 2012; Green and Akam, 2014; Hejnol and Martín-Durán, 2015; Perry et al., 2015; Satou and Imai, 2015; Martín-Durán et al., 2016; Vellutini et al., 2017; Andrikou et al., 2019). Since no mesodermal expression of *Bra* is present in the acoel *Convolutriloba longifissura*, it seems that expression of *Bra* in the mesoderm may have developed in the lineage of nephrozoans with a possible loss of function in tunicates and various clades of spiralians (Figure 11; Hejnol and Martindale, 2008a). The *Brachyury* ortholog was not found in the genome of the nematode *Caenorhabditis elegans* and the platyhelminth *Schmidtea polychroa*, implying a possible loss of the *Brachyury* gene in both taxa (Figure 11; Pocock et al., 2004; Martín-Durán and Romero, 2011; Sebé-Pedrós and Ruiz-Trillo, 2017).

To summarize, the data currently available suggest that *Brachyury* was expressed during blastopore and digestive tract development in the last common ancestor (LCA) of Bilateria. In addition, *Brachyury* was involved in mesoderm formation in the LCA of Nephrozoa, while a novel expression of *Bra* is in the ectoderm along the ventral midline in Molluska (Figure 11).

## Comparative *even-skipped* expression in Metazoa

In the gastrula stage and trochophore larva of *Dreissena rostriformis*, *eve* is found in the developing mesoderm and in the ectoderm of the shell field. These constitute the first *eve* expression data for any mollusk (Figure 12). In a number of bilaterians and the cnidarian *Nematostella vectensis*, *eve* is expressed in the ectoderm, which is commonly associated with the hindgut formation and/or neurogenesis (Figure 12; Ikuta et al., 2004; Ryan et al., 2007; Martín-Durán et al., 2016; Vellutini et al., 2017). Accordingly, ectodermal expression of *eve* seems to be a conserved feature across bilaterian taxa (Figure 12). Expression of *eve* during mesoderm formation has been documented in vertebrates and the amphioxus, as well as in the majority of protostomes, including most annelids, an ectoproct, *C. elegans* and arthropods (e.g., *Artemia franciscana* and *Drosophila*; Figure 12; Ruiz i Altaba and Melton, 1989; Ferrier et al., 2001; Seebald and Szeto, 2011; Kozin et al., 2016; Martín-Durán et al., 2016; Vellutini et al., 2017). In *A. franciscana*, *Drosophila* and *C. elegans*, *eve* is additionally expressed in mesoderm derivatives such as in muscle and/or heart cells, and *eve* expression is required for limb development in the mouse and zebrafish (Ahringer, 1996; Herault et al., 1996; Sordino et al., 1996; Copf et al., 2003; Fujioka et al., 2005). However, *eve* was not found to be expressed in the mesoderm in a few protostomes, including brachiopods, a nemertean, and a priapulid, as well as in some deuterostomes, e.g., the sea urchin embryo and the ascidian *Ciona intestinalis* (Figure 12; Ikuta et al., 2004; Li et al., 2014; Martín-Durán and Hejnol, 2015; Martín-Durán et al., 2015; Martín-Durán et al., 2016). Since *eve* is not expressed in the mesoderm of the acoel *C. longifissura*, it appears that *eve* may have a conserved role in the development of the nephrozoan mesoderm, but mesodermal expression seems to have been subject to loss in multiple lineages (Figure 12; Hejnol and Martindale, 2008b). The *even-skipped* gene is not present in the genome of the ctenophore *M. leidyi*, the placozoan *Trichoplax adhaerens*, and poriferans *Amphimedon queenslandica* and *Sycon ciliatum*, suggesting a possible loss of the

*eve* gene in all these taxa or they never had it (Figure 12; Hejnol and Martindale, 2008b; Schierwater et al., 2008; Ryan et al., 2010; Leininger et al., 2014).

Comparative analysis implies that *eve* has a conserved feature in nephrozoan mesoderm formation, derived from a more ancestral role in ectoderm development, which is shared between bilaterians and cnidarians. The ectodermal shell field expression of *eve* in *Dreissena* is an evolutionary novelty for either dreissenids, Bivalvia, or Conchifera (Figure 12).

## Comparative *Mox* expression in Metazoa

In the trochophore larva of *Dreissena rostriformis*, *Mox* is expressed in the ventral mesoderm in the region of the ventral expression of *mhc* and at the site of the ventro-posterior musculature. A similar *Mox* expression pattern is found in some lophotrochozoans such as the gastropod *Haliotis asinina* and the annelid *Alitta virens*, as well as in most chordates, including the ascidian *C. intestinalis* and several vertebrates, where *Mox* is expressed during mesoderm formation and is involved in myogenesis (Figure 13; Candia and Wright, 1995; Mankoo et al., 1999; Neyt et al., 2000; Rallis et al., 2001; Hinman and Degnan, 2002; Ikuta et al., 2004; Satou and Imai, 2015; Kozin et al., 2016). *Mox* expression in the mesoderm has been reported in almost all investigated taxa of protostomes and deuterostomes, suggesting that *Mox* may have an ancestral role in bilaterian mesoderm development (Figure 13; Chiang et al., 1994; Minguillón and Garcia-Fernàndez, 2002; Lowe et al., 2006; Passamaneck et al., 2015; Andrikou et al., 2020). Moreover, it appears that *Mox* may also have an ancestral feature in bilaterian myogenesis, however, more *Mox* expression data with comparative data on muscle development are required to unequivocally settle this issue. In the sea urchin embryo, *Mox* is only involved in neurogenesis, which was also found in late stages of *Drosophila*, but *Mox* is also expressed in the mesoderm in the latter (Figure 13; Chiang et al., 1994; Poustka et al.,

2007). It appears likely that *eve* expression in neural cells may have developed independently in lineages to echinoderms and arthropods (Figure 13). In the anthozoan *N. vectensis* and hydrozoan *Clytia hemisphaerica*, *Mox* is expressed in the pharyngeal endoderm, which supports that *Mox* may have an ancestral role in mesoderm formation in bilaterian animals (Figure 13; Ryan et al., 2007; Chiori et al., 2009). By contrast, the *Mox* gene was not found in the genome of *C. elegans*, the ctenophore *M. leidyi*, the placozoan *T. adhaerens*, and the poriferan *A. queenslandica*, indicating a possible loss of the *Mox* gene or the last three mentioned taxa never had it (Figure 13; Ruvkun and Hobert, 1998; Schierwater et al., 2008; Ryan et al., 2010).

Taken together, the data presently available suggest that *Mox* was involved in mesoderm formation and might be in myogenesis in the LCA of Bilateria with a complete loss of *Mox* expression in the mesoderm in echinoderms (Figure 13).

## Comparative larval myoanatomy in Bivalvia

Five distinct muscle systems are present in the veliger larva of *Dreissena rostriformis,* namely the velum muscle ring, four pairs of velum retractors, one pair of ventral larval retractor, one pair of foot retractor, the mantle musculature including the muscles of the pallial line and two pairs of mantle retractors and an initially paired anterior adductor. A posterior adductor muscle and the pedal plexus (foot), as present in the adult, were not found, which most likely emerges in late larva stages or after metamorphosis.

The velum muscle ring degenerates prior to or at metamorphosis and has been reported in only a few bivalve lineages, including dreissenids, teredinids, and mytilids (Figure 14A; Dyachuk and Odintsova 2009; Wurzinger-Mayer et al., 2014; Kurita et al., 2016; present study). Interestingly, this muscle ring was not found in most bivalve larvae (Figure 14A; Audino et al., 2015; Wurzinger-Mayer et al., 2014; Wanninger and Wollesen, 2015; Li et al., 2019; Sun et al.,

2020). However, since the prototroch/velum muscle ring occurs in almost all class-level sublineages of mollusks with indirect development except for the scaphopods, it seems most likely that it is part of the molluskan larval muscular ground pattern (Figure 14A; Wanninger and Wollesen, 2015).

The velum retractors have been documented in all veliger larvae of autobranch bivalves investigated to date and are resorbed prior to or during metamorphosis. But the number differs between species, e.g., four pairs are common in euheterodonts, except in the teredinid shipworm *Lyrodus pedicellatus*, where two pairs are present (Figure 14A; Wurzinger-Mayer et al., 2014; Wanninger and Wollesen, 2015; present study). Interestingly, the two pairs of the shipworm were supposed to transform into the future mantle musculature. However, this condition has not been described for any other mollusk and, if true, most likely constitutes an apomorphy of this genus or species (Wurzinger-Mayer et al., 2014). In pteriomorph larvae, four pairs of velum retractors were found in pectinids, whereas three pairs are present in oysters and two to three pairs were described in mytilids (Figure 14A; Cragg, 1985; Dyachuk and Odintsova, 2009; Audino et al., 2015; Kurita et al., 2016; Li et al., 2019; Sun et al., 2019; Sun et al., 2020). To summarize, three or four pairs of velum retractors appear most likely to be a part of the myoanatomy ground pattern in autobranch bivalve larvae (Figure 14). Nevertheless, the velum retractors of bivalves seem likely to be homolog to that of gastropods (also called main retractors) because of the same location and structure (Wanninger and Wollesen, 2015). This suggests that the ancestral muscular condition of bivalve larvae contains likely at least one pair of velum retractors (Figure 14A).

The larval retractors disappear prior to or at metamorphosis and have been reported in most autobranch bivalve lineages, even in the semi-direct (brooding) lasaeids (Wurzinger-Mayer et al., 2014; Wanninger and Wollesen, 2015). However, the number of larval retractors differs among species, e.g., one (ventral) pair is common in imparidents, except in the lasaeids which

contain three pairs, while in pteriomorphs, one to five pairs are present (Figure14A; Wurzinger-Mayer et al., 2014; Audino et al., 2015; Kurita et al., 2016; Wanninger and Wollesen, 2015; Li et al., 2019; Sun et al., 2020; present study). Accordingly, one or two pairs of larval retractors appear most likely to be a part of the muscular ground pattern in the autobranch bivalve larvae (Figure 14).

A dimyarian condition, including the anterior and the posterior adductor, has been documented in many adult bivalves. In adult pectinids and oysters, a monomyarian arrangement with only one adductor is present (Giribet, 2008; Salvini-Plawen and Haszprunar, 2013; Cragg, 2016; Li et al., 2019). The anterior and the posterior adductor were found in most bivalve larvae, including protobranchs and autobranchs, even in pectinids and oysters, where the anterior adductor begins to disintegrate during metamorphosis (Figure 14A; Drew, 1899; Drew, 1901; Wurzinger-Mayer et al., 2014; Audino et al., 2015; Wanninger and Wollesen, 2015; Li et al., 2019; Sun et al., 2019; Sun et al., 2020). Interestingly, a transient larval adductor is present in the parasitic glochidium larva of unionids, while the anterior and the posterior adductor of adults appear to develop independently during the development (Hebers, 1913). In veliger larvae of some imparidents such as dreissenids and teredinids as well as most pteriomorphs, an initially two-partite condition of the anterior adductor has been described in the early development (Figure 14A; Wurzinger-Mayer et al., 2014; Audino et al., 2015; Li et al., 2019; Sun et al., 2019; present study). Taken together, these data show that the anterior and the posterior adductor are most likely a part of the bivalve larval muscular ground plan (Figure 14A). The two-part arrangement of the anterior adductor throughout autobranchs might indicate a paired anterior adductor in the last LCA of Autobranchia or even the entire Bivalvia (Figure 14A).

The adult muscles of the pallial line have been reported to emerge in many autobranch bivalve larvae (Figure 14A; Wurzinger-Mayer et al., 2014; Audino et al., 2015; Li et al., 2019; Sun et

al., 2019; Sun et al., 2020; present study). However, the mantle retractors of bivalves show a difference in the numbers and the time of emergence. In most pteriomorphs, such as many pectinids, oysters, and the mytilid *Mytilus trossolus*, several pairs of mantle retractors are formed after metamorphosis (Figure 14A; Dyachuk and Odintsova, 2009; Li et al., 2019; Sun et al., 2020). Similar mantle retractors are originated during late larval stages in the pectinid *Nodipecten nodosus* and the semi-direct lasaeid *Lasaea adansonii* (Figure 14A; Altnöder and Haszprunar, 2008; Audino et al., 2015). In most imparidents, including dreissenids, montacutids, and teredinids, the mantle retractors are emerged during larval stages, but the number differs among species, e.g., two pairs are present in dreissenids and montacutids, while three pairs were found in the teredinids (Figure 14A; Wurzinger-Mayer et al., 2014; Wanninger and Wollesen, 2015; present study). However, it is not clarified whether these mantle retractors of imparidents are retained after metamorphosis and data of advanced juveniles are needed to unequivocally settle this issue. Accordingly, the myoanatomy ground pattern of autobranch bivalve larvae contains most likely the muscles of the pallial line and possibly at least two mantle retractors (Figure 14).

The foot retractors together with the plexus-like foot musculature are preferred muscles of the adult foot muscle system and have been documented to be formed in most bivalve larvae investigated so far (Figure 14A; Wurzinger-Mayer et al., 2014; Audino et al., 2015; Li et al., 2019; Sun et al., 2020). However, the number of foot retractors differs among species of bivalve larvae, e.g., two pairs are common in autobranchs (see Table 2 of Wurzinger-Mayer et al., 2014), while one pair is present in dreissenids and montacutids (Figure 14A; Wanninger and Wollesen, 2015; present study). In veliger larvae of the mytilid *Septifer virgatus*, a putative anlage of the pedal plexus, but no foot retractors were found, however, data of late stages are required in order to settle this issue (Figure 14A; Kurita et al., 2016). In the mytilid *M. trossolus*, the foot musculature emerges after metamorphosis (Figure 14A; Dyachuk and Odintsova,

2009). Interestingly, adult oysters have no foot, but distinct muscles of the foot retractors and the pedal plexus occur in veliger larvae of *Crassostrea gigas* and are lost completely after metamorphosis (Figure 14A; Li et al., 2019). In summary, two pairs of foot retractors together with the plexus-like foot musculature seem most likely to be a part of the autobranch bivalve muscular ground pattern (Figure 14).

The comparative analysis suggests that at least a velum muscle ring, three or four pairs of velum retractors, one or two pairs of larval retractors, an anterior and a posterior adductor, two pairs of foot retractors together with the plexus-like foot musculature, as well as the mantle musculature including muscles of the pallial line and possibly two pairs of mantle retractors are part of the muscular ground pattern of autobranch bivalve larvae (Figure 14). The two-partite condition of the anterior adductor in early development throughout Autobranchia might argue for a paired anterior adductor in the LCA of autobranchs or even the entire Bivalvia (Figure 14). Moreover, the current data show that at least a velum muscle ring, a pair of velum retractors, the anterior and the posterior adductor were present in the LCA of bivalve larvae (Figure 14A). For further assessments concerning the ground plan of entire Bivalvia, more data on the earliest branching Protobranchia are required.

## Conclusion

The present study shows that mesodermal expression of *Dro-Bra*, *Dro-eve* and *Dro-Mox* are congruent with the situation in most other taxa, suggesting that *Mox* has an ancestral role in bilaterian mesoderm formation, while *even-skipped* as well as *Brachyury* have a conserved feature in mesoderm development along nephorozoan lineages. The available data of bivalve myogenesis indicate that the muscular ground pattern of autobranch bivalve larvae contains five muscle systems. Furthermore, the major adult muscles originate prior to metamorphosis.

**Acknowledgements**

I would like to thank my supervisor Andreas Wanninger for providing this interesting topic, which contained different methods. Furthermore, he supported me the whole time of my master thesis, which included different presentations and talks of my work, e.g., the 1st MoFA (Mollusk Research Austria) Meeting in Salzburg, Young Researcher Meeting Morphology in Vienna and different seminars of the University of Vienna. Additionally, I am grateful for various scientific discussions, talks, and writing tips.

I want to thank Livia Rudoll for the instruction of the safety training in the different labs. Many thanks to Elisabeth Zieger and Andrew Calcino to instructed me, how I can carry out a controlled spawning and, subsequently, how I can handle a larvae culture in the lab for a longer time. Moreover, I would like to thank Elisabeth Zieger for her helpful instructions in laboratory techniques. I am grateful to Andrew Calcino for the training in bioinformatic analyses. Furthermore, many thanks to Elisabeth Zieger and Cristian Baranyi for the helpful instructions in the molecular labs. For the training of the WMISH, I want to thank David Salamanca. Moreover, I would like to thank Thomas Schwaha for showing me how to use the CLSM as well as different software programmes, e.g., ImageJ2, Imaris x64, and Inkscape.

A big thanks to my roommates David Salamanca and Atilla Sachslehner, who always had time for different discussions about scientific stuff. Let me also thank the whole workgroup of Andreas Wanninger which always had time for questions, discussions and gave me suggestions for my work. Furthermore, it was a very nice time in the Department of Evolutionary Biology (Unit Integrative Zoology), and I learned a lot of scientific work.

## Figures

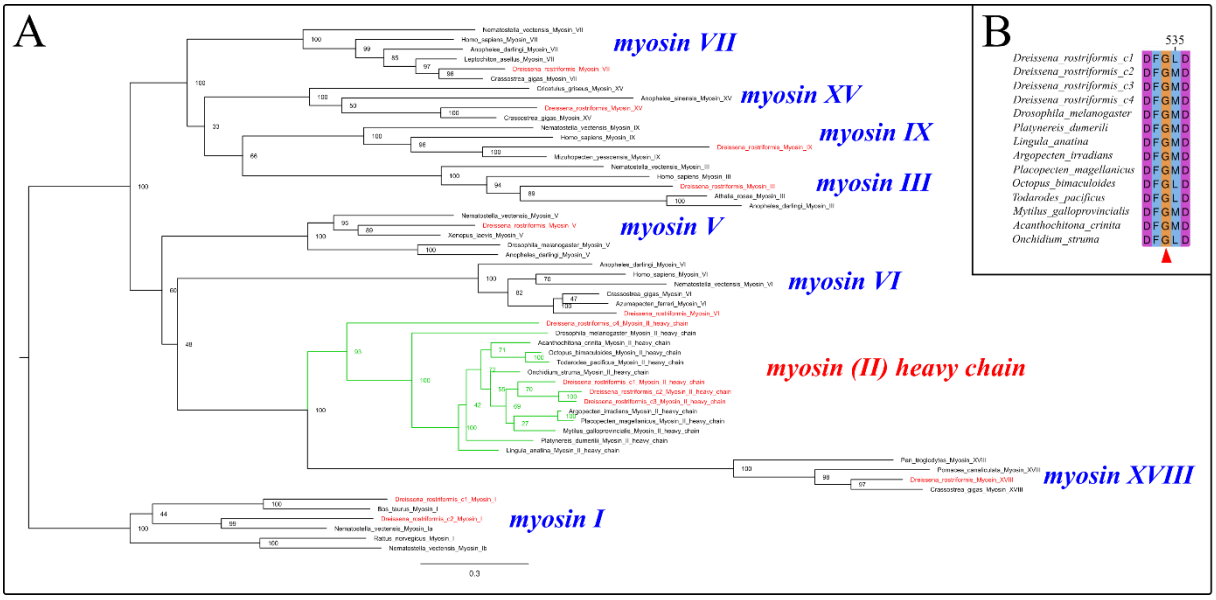


**Figure 1.** Phylogenetic analysis of all annotated genes with a myosin head domain in *Dreissena rostriformis*. A: Phylogenetic tree of relevant metazoan-specific *myosin* families. *Myosin I* is used as outgroup. Thirteen candidates of *D. rostriformis* (marked in red) nest within the following gene families: *myosin I*, *myosin II heavy chain*, *myosin III*, *myosin V*, *myosin VI*, *myosin VII*, *myosin IX*, *myosin XV, myosin XVIII*. B: Clipped alignment of the *myosin II heavy chain* family showing the specific Glycine (G) (red arrowhead).

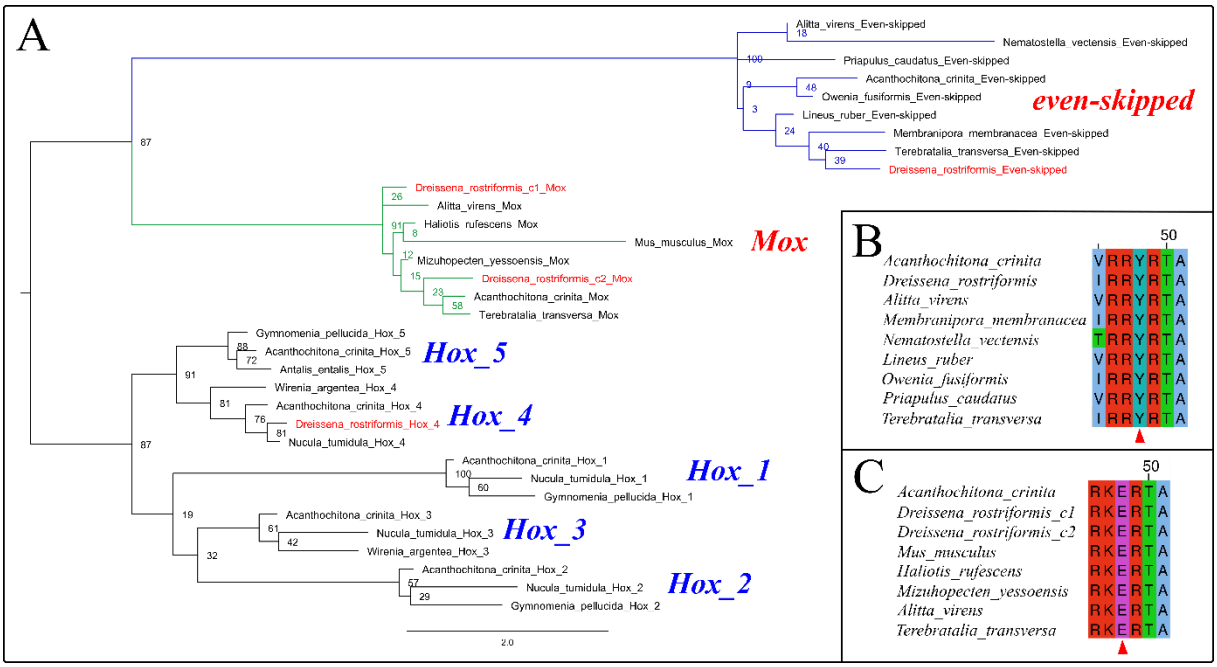


**Figure 2.** Phylogenetic analysis of *even-skipped* (*eve*) and *Mox* genes in *Dreissena rostriformis*. A: Phylogenetic tree of *eve* and *Mox* genes with *Hox* genes used as outgroup. All sequences contain a homeodomain. *Dreissena eve* and *Mox* genes (marked in red) nest within the corresponding gene family. The third *Mox* candidate nests within the *Hox4* family. B: Detailed alignment of the *eve* family showing the specific tyrosine (Y) (red arrowhead) at position 48. C: Clipped alignment of the *Mox* family showing a specific glutamic acid (E) (red arrowhead) at position 48. B, C: In both families, the specific amino acids are at the beginning of the homeodomain.

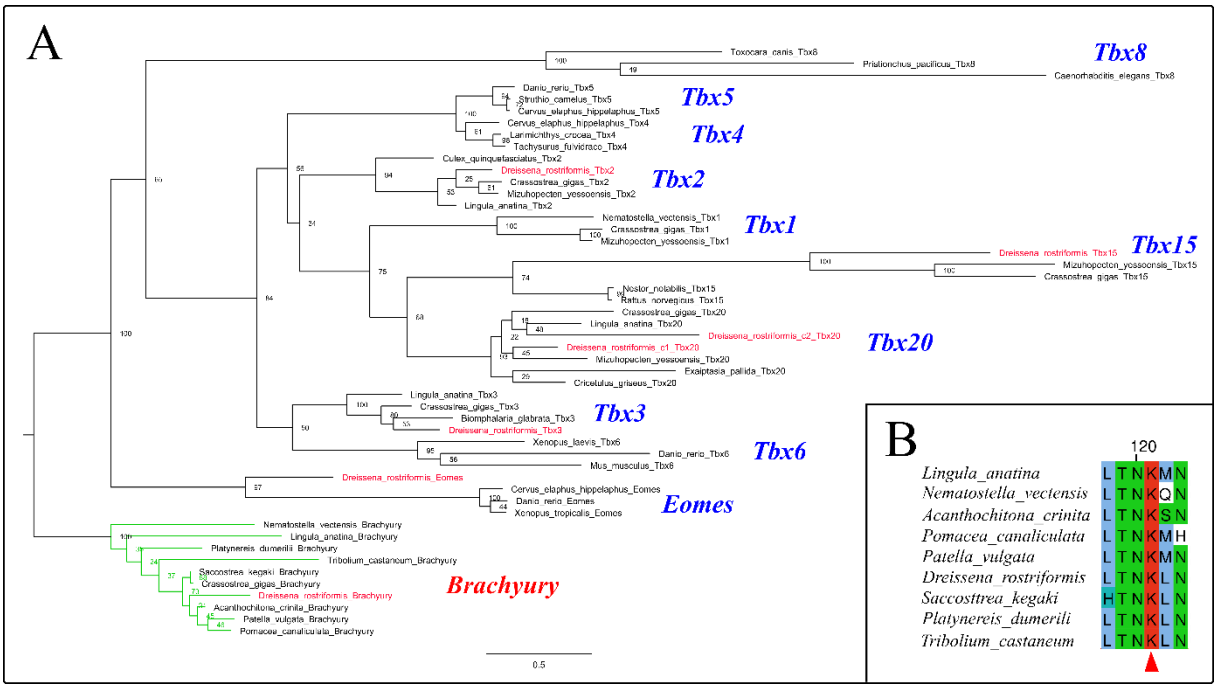


**Figure 3.** Phylogenetic analysis of all annotated *Dreissena rostriformis* genes containing a T-box domain. A: Phylogenetic tree with all metazoan-specific T-box families with *Brachyury* used as outgroup. Seven candidates of *D. rostriformis* (marked in red) nest within the following gene families: *Brachyury*, *Eomes*, *Tbx2*, *Tbx3*, *Tbx15*, *Tbx20*. B: Detailed alignment of the *Brachyury* family showing the specific Lysine (K) (red arrowhead) at position 121 within the T-box domain.

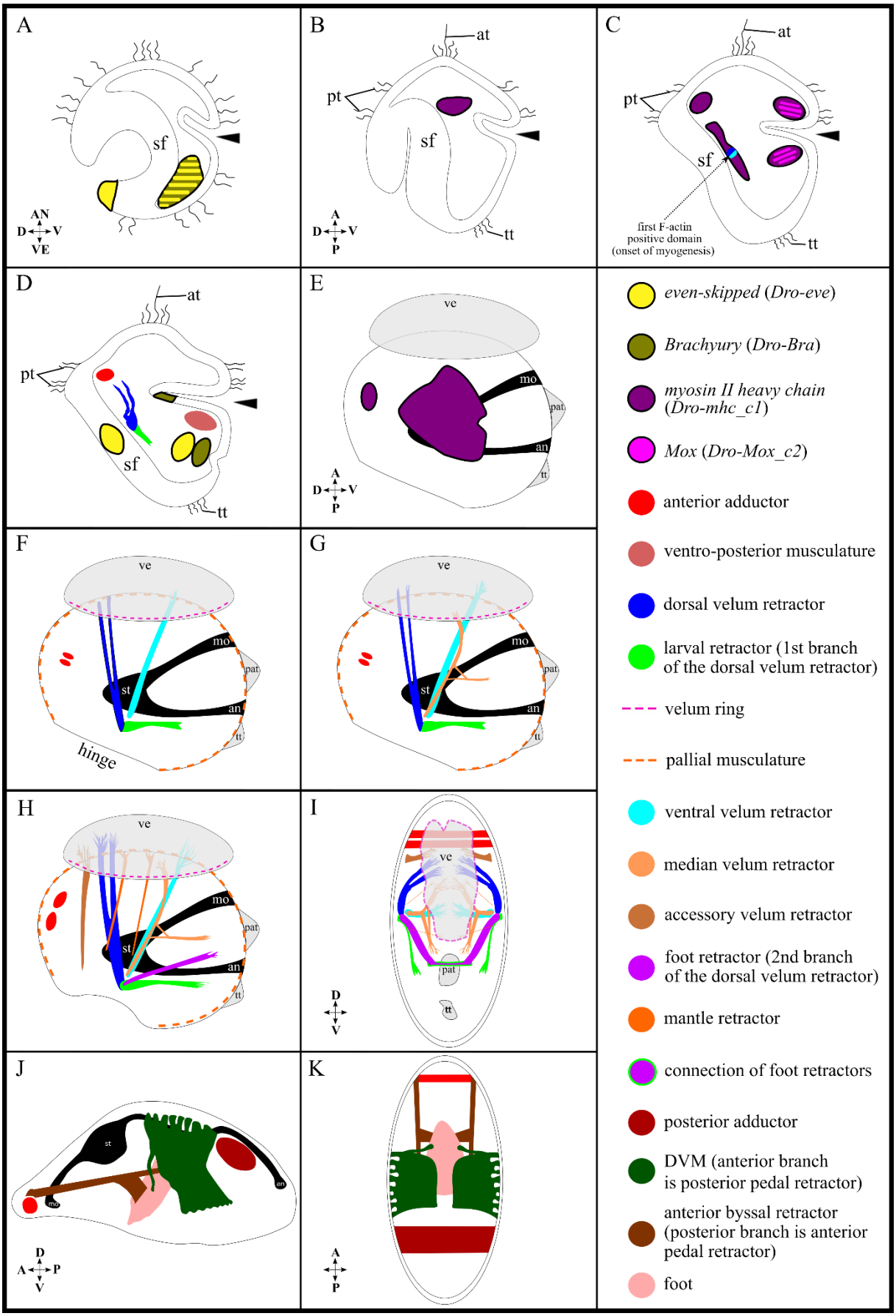
A
sf
AN
D
V
VE
B
at
pt
sf
tt
C
at
pt
sf
first F-actin
positive domain
(onset of myogenesis)
tt
D
at
pt
sf
tt
E
ve
mo
pat
an
tt
F
ve
mo
pat
st
an
tt
hinge
G
ve
mo
pat
st
an
tt
H
ve
mo
pat
st
an
tt
I
ve
pat
tt
J
st
mo
an
K
even-skipped (Dro-eve)
Brachyury (Dro-Bra)
myosin II heavy chain (Dro-mhc_c1)
Mox (Dro-Mox_c2)
anterior adductor
ventro-posterior musculature
dorsal velum retractor
larval retractor (1st branch of the dorsal velum retractor)
velum ring
pallial musculature
ventral velum retractor
median velum retractor
accessory velum retractor
foot retractor (2nd branch of the dorsal velum retractor)
mantle retractor
connection of foot retractors
posterior adductor
DVM (anterior branch is posterior pedal retractor)
anterior byssal retractor (posterior branch is anterior pedal retractor)
foot

**Figure 4.** Schematic summary of gene expression and myogenesis of developmental stages in *Dreissena rostriformis*. Lateral view in all images which anterior/animal is up and dorsal is left except I which is an anterior view and K which is a dorsal view. A (anterior), AN (animal), an (anus), apical tuft (at), black arrowheads (blastopore/stomodaeum), D (dorsal), mo (mouth), P (posterior), pre-anal tuft (pat), prototroch (pt), sf (shell field), st (stomach), telotroch (tt), V (ventral), VE (vegetal), ve (velum). A: Ciliated gastrula with mesodermal expression of *Brachyury* (*Bra*) and *even-skipped* (*eve*), and ectodermal expression of *eve*. B: Trochophore larva with mesodermal expression of *myosin II heavy chain* (*mhc*). C: Older trochophore larva as in B showing mesodermal expression of *Mox* and *mhc*, and the first F-actin positive domain. D: Trochophore larva with gene expression in the mesoderm (*Bra*, *eve*), endoderm (*Bra*) and ectoderm (*eve*). In addition, first appearance of developing muscles: dorsal velum retractor, larval retractor, anlage of the anterior adductor and ventro-posterior musculature. E: D-shaped veliger larva with *mhc* expression in the dorsal and central mesoderm. F: Same stage as in E showing first distinct muscle bundles: dorsal velum retractor, ventral velum retractor, larval retractor, velum muscle ring, pallial musculature, and two-partite anterior adductor. G: Slightly older stage as in F with a median velum retractor. H: Late veliger larva with additional muscles: accessory velum retractor, foot retractor, and two mantle retractors. I: Slightly older stage as in H showing the connection of both foot retractors. J and K: Musculature of an adult mussel (adapted from Nalepa and Schloesser, 1993) including the anterior and the posterior adductor, the dorsal-ventral musculature (DVM), the anterior byssal retractor and the foot.

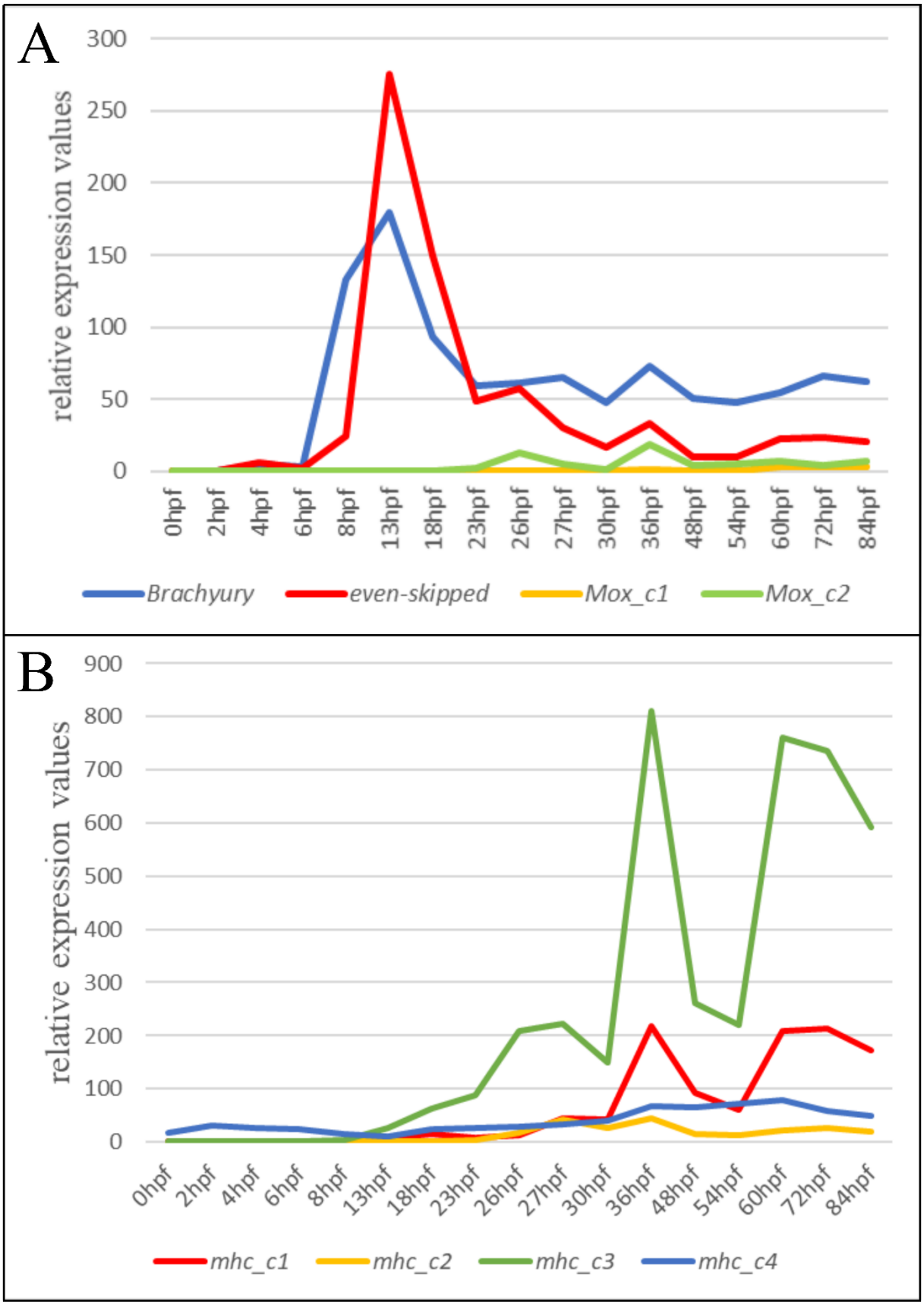


**Figure 5.** Relative gene expression values of selected genes of *Dreissena rostriformis*. C (candidate). The x-axis provides different stages, which are given in hours post fertilisation

(hpf). The y-axis presents relative values (also in Table 5) of the gene expression levels in different stages. A: *Brachyury* (blue) and *even-skipped* (red) show high relative expression values during early stages. Relative expression values of *Mox_c1* (yellow) are very low, with the highest peak at 72 hpf. *Mox_c2* (green) presents low relative expression values with two high peaks at 26 hpf and 36 hpf. B: All annotated *myosin II heavy chain* (*mhc*) candidates of *D. rostriformis* show the highest expression after 30 hpf.

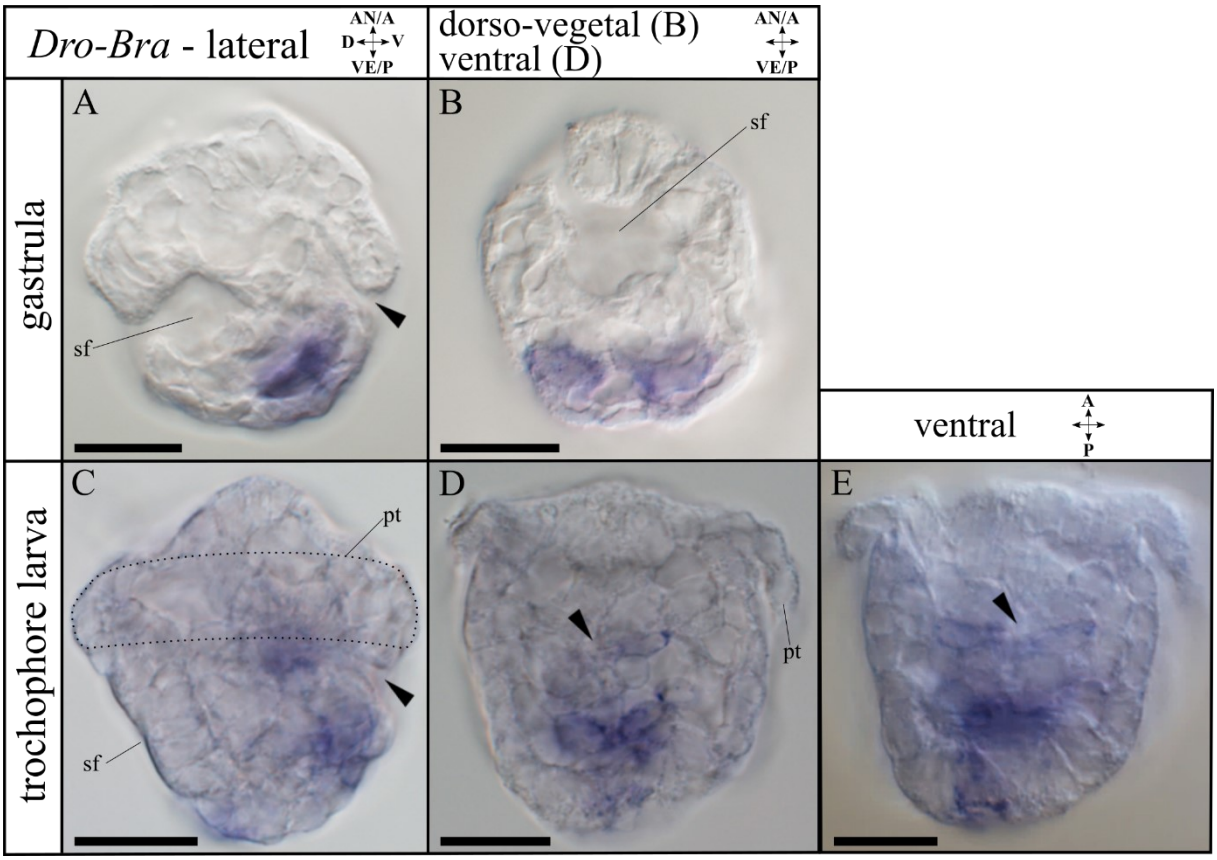


**Figure 6.** Expression of *Brachyury* (*Dro-Bra*) in *Dreissena rostriformis* gastrula and trochophore stages. Animal (A, B) and anterior (C-E) is up. Black arrowheads indicate the blastopore/stomodaeum, sf marks the shell field, dotted line presents the region of the prototroch (pt). Scale bar equals 20 µm. A: *Dro-Bra* expression is first present in the mesoderm at the ventral region. B: Ventral mesodermal expression of *Dro-Bra*. C: *Dro-Bra* is expressed in the ventro-posterior mesoderm and endodermally in the developing foregut. D: Mesodermal and endodermal expression of *Dro-Bra*. The left and right lobes belong to the prototroch (pt). E: A different focal plane as in D with a focus on the endodermal *Dro-Bra* expression. A, anterior; AN, animal; D, dorsal; P, posterior; V, ventral; VE, vegetal.

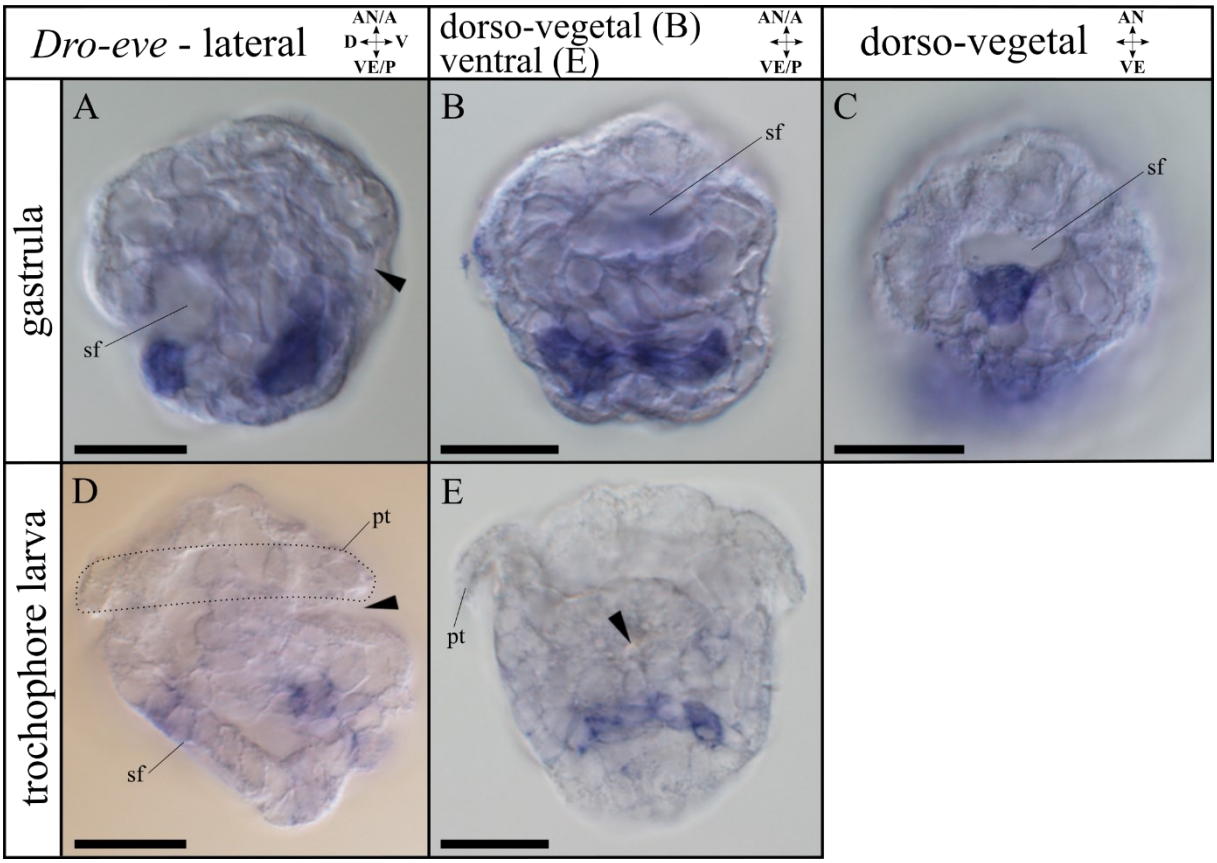


**Figure 7.** Expression of *even-skipped* (*Dro-eve*) during early development in *Dreissena rostriformis*. Animal (A-C) and anterior (D, E) is up, black arrowheads indicate the blastopore/stomodaeum, dotted line marks the region of the prototroch, sf indicates the shell field. Scale bar equals 20 µm. A: *Dro-eve* is first expressed in the mesoderm at the ventral region and ectodermally in the shell field at the gastrula stage. B: Mesodermal expression of *Dro-eve* in the ventral region. C: Ectodermal expression of *Dro-eve* in the shell field. D: *Dro-eve* expression is located in the ventro-posterior mesoderm and in the ectoderm of the shell field in the trochophore larva. E: Mesodermal expression of *Dro-eve* in the ventro-posterior region. The lobes on the sides of the trochophore larva indicate the prototroch (pt). A, anterior; AN, animal; D, dorsal; P, posterior; V, ventral; VE, vegetal.

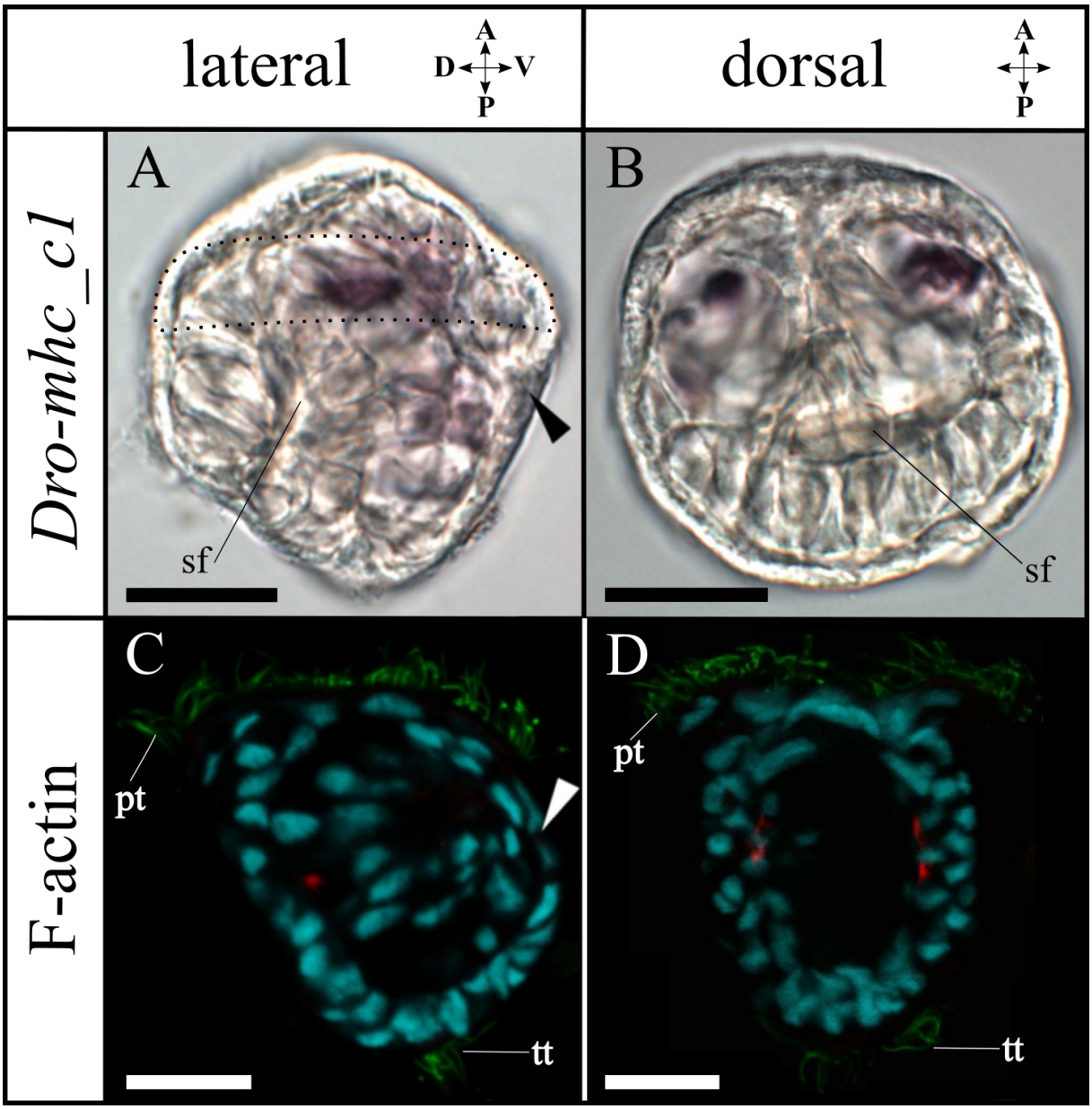


**Figure 8.** Expression of *myosin II heavy chain* (*Dro-mhc_c1*) and immunofluorescence staining in *Dreissena rostriformis* trochophore larvae. Anterior is up. Arrowheads indicate the stomodaeum, sf marks the shell field, dotted line indicates the region of the prototroch (pt). Scale bar equals 20 µm. Brightfield images (A, B) of the gene expression and confocal images (C, D) with F-actin (red), cilia (green; pt: prototroch; tt: telotroch) and cell nucleus (cyan) staining. A: *Dro-mhc_c1* expression is first present in the anterior mesoderm. B: Mesodermal expression of *Dro-mhc_c1* in the anterior region. C: First F-actin-positive domain in the mesoderm below the shell field at the dorso-median region. D: Slightly further developed

trochophore larva showing two developing myofilaments/muscle fibres (F-actin positive domains) in the median region. A, anterior; D, dorsal; P, posterior; V, ventral.

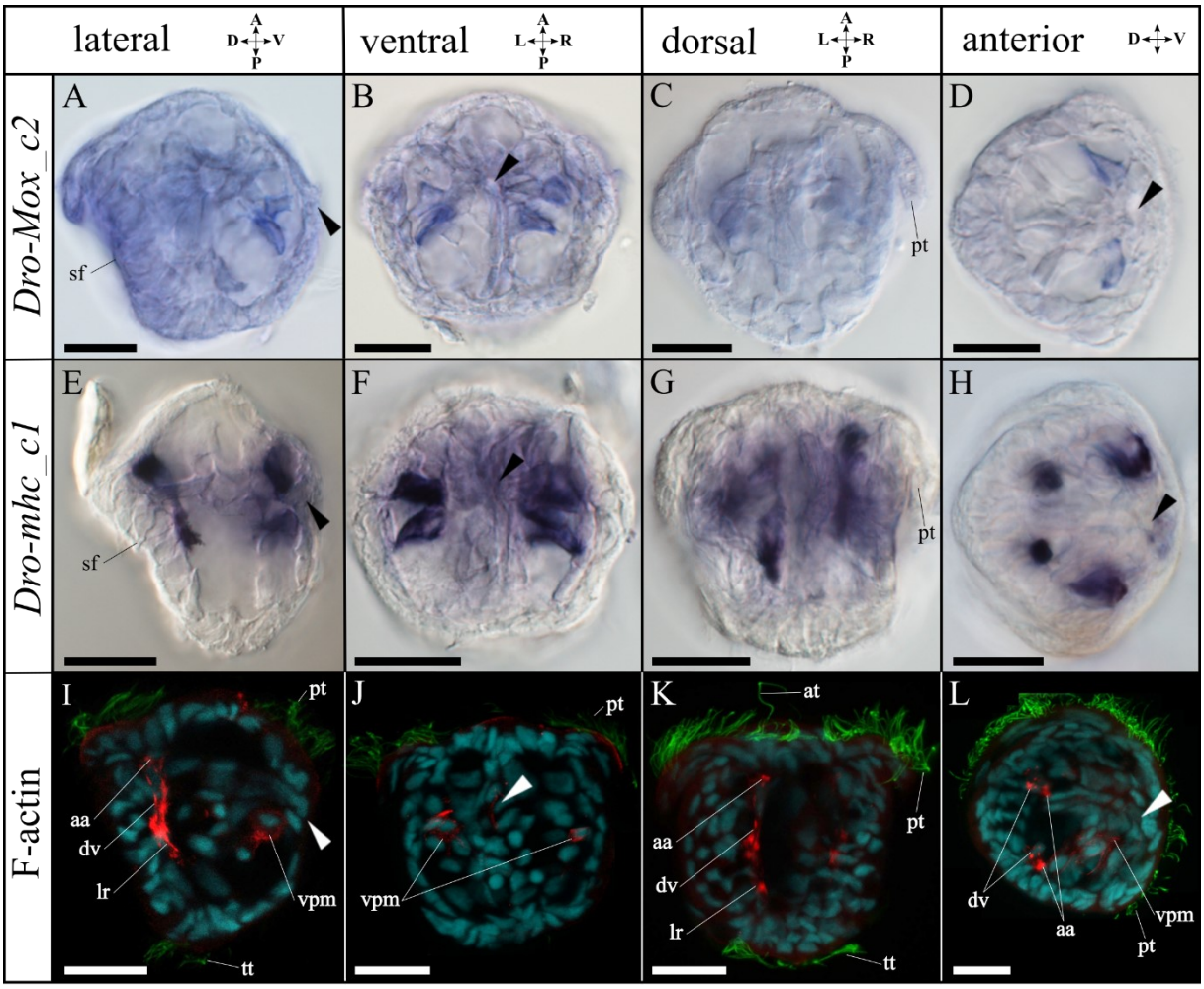


**Figure 9.** Expression of *Mox* (*Dro-Mox_c2*) and *myosin II heavy chain* (*Dro-mhc_c1*) and immunofluorescence staining in *Dreissena rostriformis* trochophore larvae. Anterior is up in all images except D, H and L, which are anterior views, arrowheads indicate the stomodaeum, sf marks the shell field. Scale bar equals 20 µm. Brightfield images (A-H) of the gene expression and confocal images (I-L) with F-actin (red), cilia (green; at: apical tuft; pt: prototroch; tt: telotroch) and cell nucleus (cyan) staining. A: Two ventral mesodermal expression domains of *Dro-Mox_c2*. B: *Dro-Mox_c2* is expressed adjacent to and posterior of the developing digestive tract, on either side. C: No expression of *Dro-Mox_c2* in the dorsal region. The lobes on the sides of the trochophore larva indicate the prototroch (pt). D: Mesodermal expression of *Dro-Mox_c2* on the ventral side. E: *Dro-mhc_c1* is expressed in the dorsal and ventral mesoderm. F: Four ventral mesodermal expression domains of *Dro-mhc_c1*.

G: Two spot-like and two stripe-like mesodermal expression domains of *Dro-mhc_c1*. H: Mesodermal expression of *Dro-mhc_c1* at the dorsal and ventral region I: First myofilaments consisting of the developing larval retractor (lr) and dorsal velum retractor (dv), and the anlage of the anterior adductor (aa) are in the dorsal region. The ventro-posterior musculature (vpm) is on the ventral side. J: A pair of the ventro-posterior musculature. K: Developing retractors (dv, lr) and the anlagen of the anterior adductors. L: Anterior view with different developing muscles as described in I. A, anterior; D, dorsal; P, posterior; V, ventral.

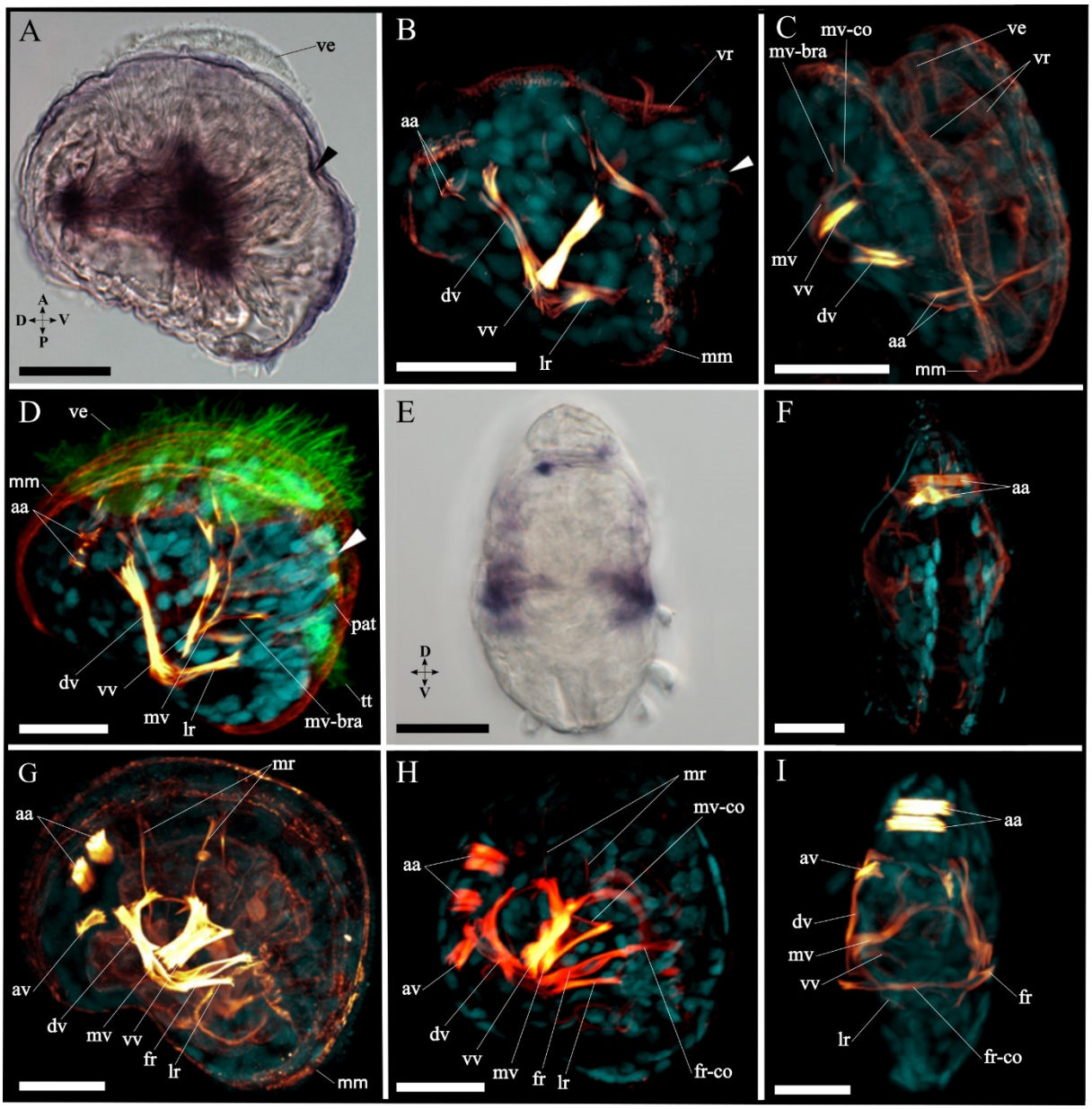


**Figure 10.** Expression of *myosin II heavy chain* (*Dro-mhc_c1*) and immunofluorescence staining in *Dreissena rostriformis* veliger larvae. Lateral view for all images, which anterior is up, dorsal is left except C which is a dorso-anterior view, E and F which are anterior views (dorsal is up) and I which is a posterior view (dorsal is up). Arrowheads indicate the stomodaeum. Scale bar equals 20 µm. Brightfield images of the gene expression (A and E) and confocal images (B-D and F-I) with F-actin (glow), cilia (green) and cell nucleus (cyan) staining. A: Expression of *Dro-mhc_c1* is in the central and dorsal mesoderm. Velum (ve). B: First distinct muscle bundles are the dorsal velum retractor (dv), the ventral velum retractor

(vv), and the larval retractor (lr). First appearance of the velum muscle ring (vr), the (pallial) muscles around the mantle margin (mm), and the merged anterior adductors (aa). C: A slightly older D-shaped veliger larva as in B showing the median velum retractor (mv) with a branch (mv-bra) and interconnection (mv-co). D: Same stage as in C with the typical cilia on the velum (ve), pre-anal tuft (pat), and telotroch (tt). E: Mesodermal expression of *Dro-mhc_c1* in the dorsal region and lateral on both sides in the median region of the D-shape veliger larva. F: Late veliger larva with prominent anterior adductors (aa). G: Same stage as in F showing the foot retractor (fr), the accessory velum retractor (av) and two mantle retractors (mr). In addition, all muscles are present as described in B and C. H: Slightly older late veliger larva as in G showing the connection of the foot retractors (fr-co) in the median plane. I: Same stage as in H. A, anterior; D, dorsal; P, posterior; V, ventral.

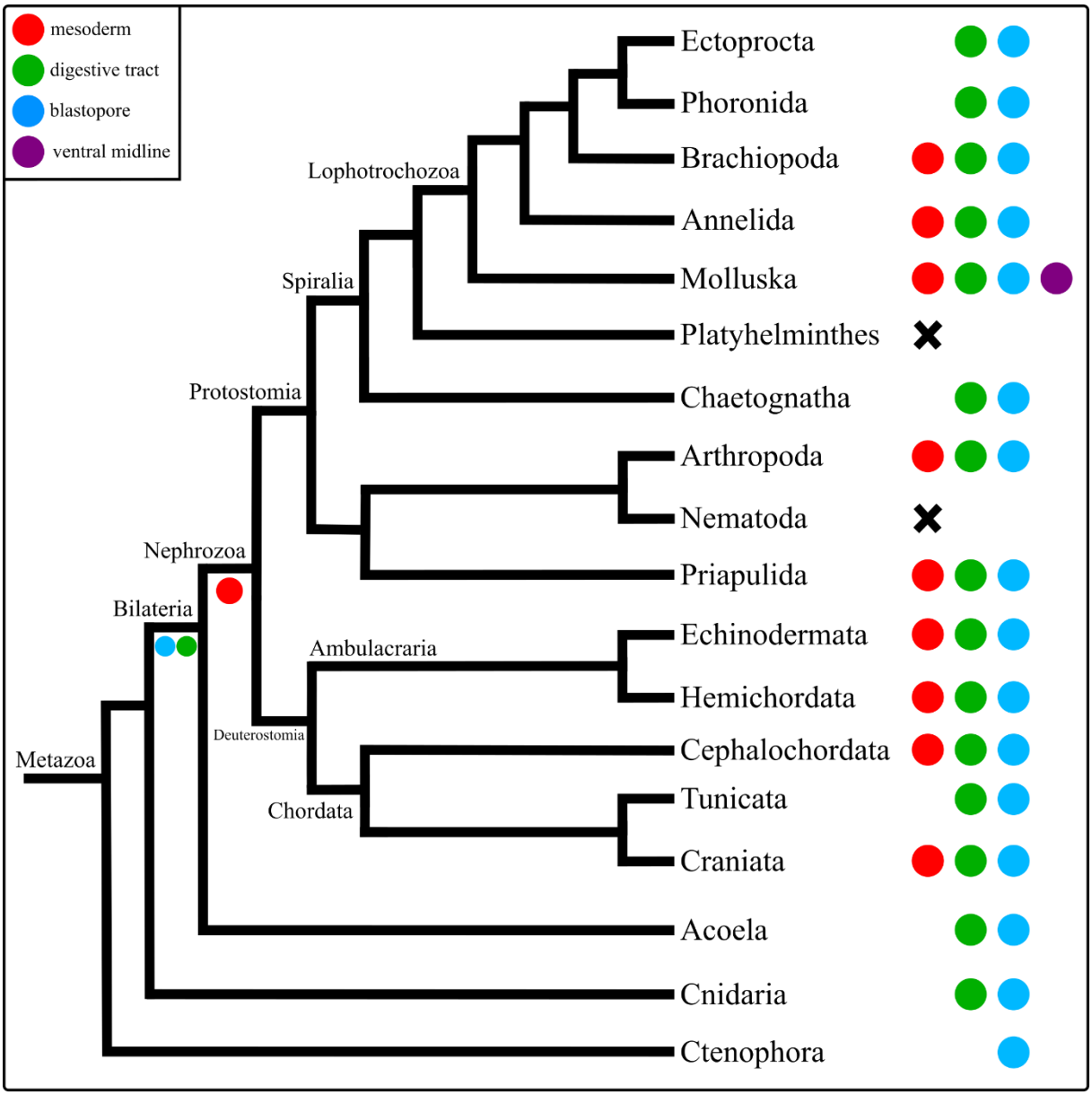


**Figure 11.** Expression of *Brachyury* (*Bra*) in metazoan lineages. X indicates that the *Brachyury* ortholog was not found in the genome. The simplified metazoan tree is adapted from Figure 1a of Laumer et al., 2019. Comparative analysis implies that *Bra* has a conserved feature in digestive tract and blastopore development among bilaterian animals with an additional conserved role in mesoderm formation in nephrozoan lineages. In addition, the expression of *Bra* in the ectoderm along the ventral midline is a novelty in mollusks. See main text for references.

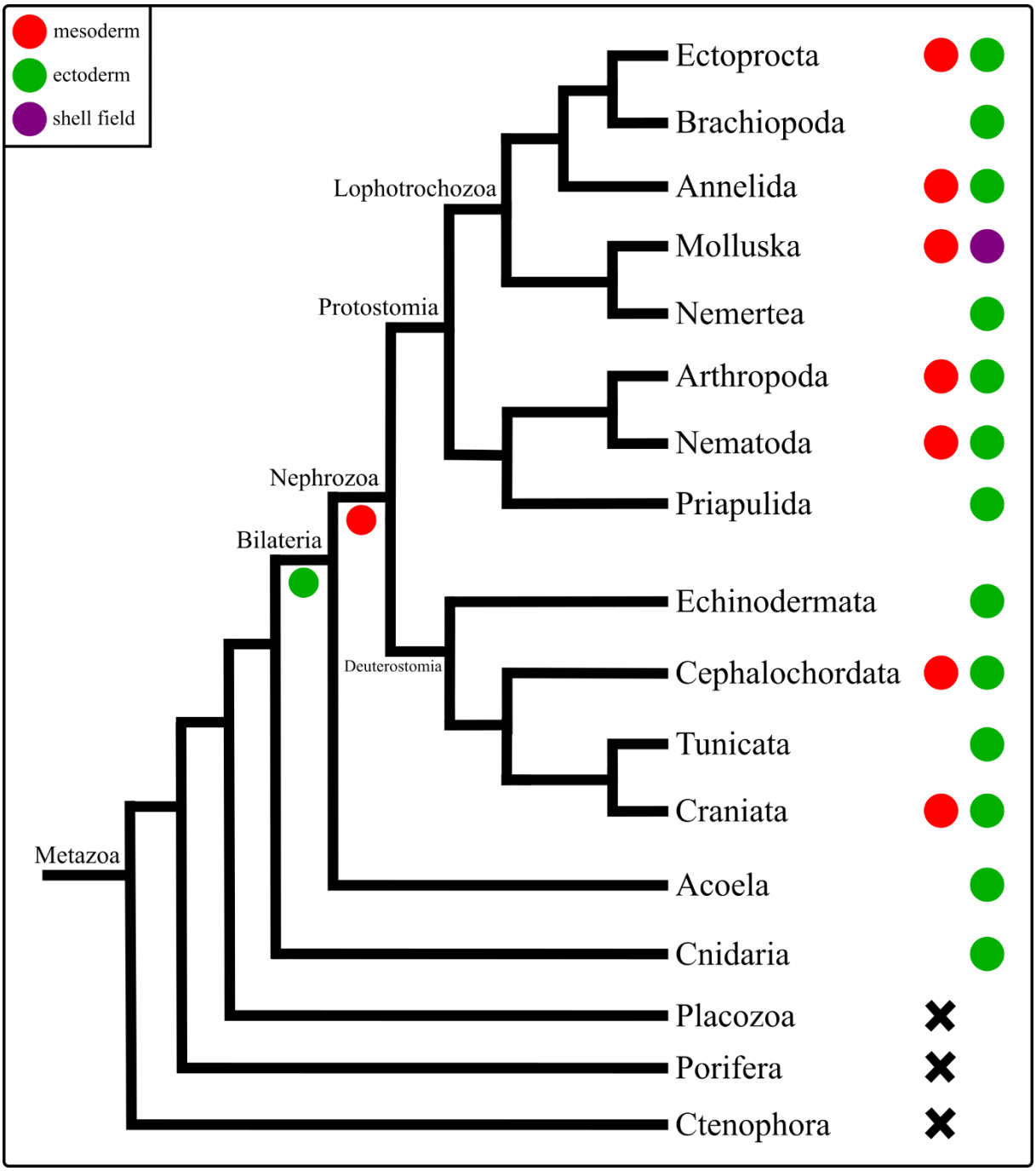


**Figure 12.** Comparative *even-skipped* (*eve*) expression in metazoans. X (not found in the genome). The data currently available indicate that *eve* was expressed during ectoderm development in the last common ancestor (LCA) of Bilateria, while *eve* was additionally involved in mesoderm formation in the LCA of Nephrozoa. Expression of *eve* in the ectodermal shell field is an evolutionary novelty of Molluska. See main text for references. The simplified metazoan tree is adapted from Figure 1a of Laumer et al., 2019.

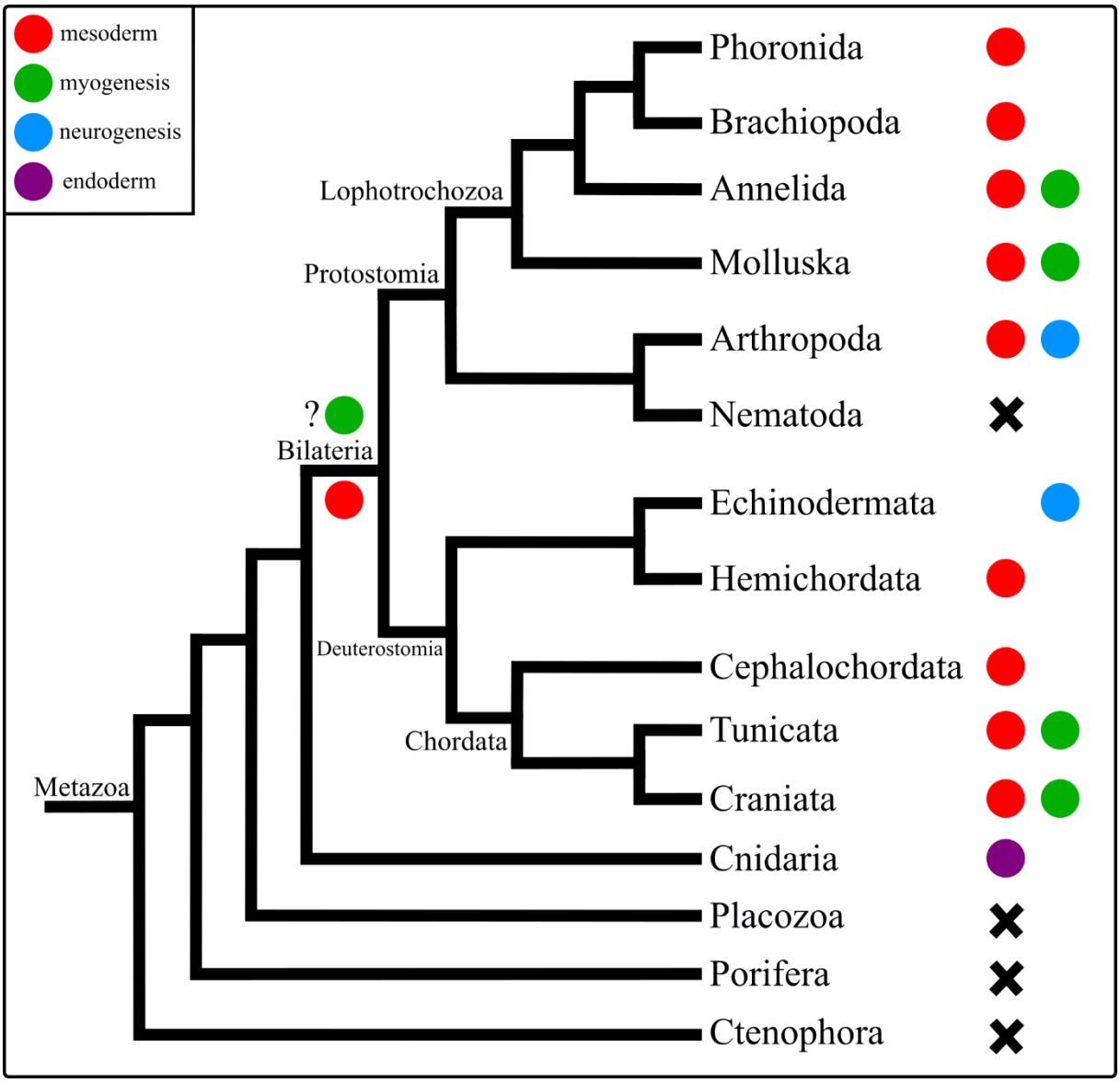


**Figure 13.** Expression of *Mox* in metazoan clades. X indicates that the *Mox* ortholog was not found in the genome. Comparative analysis suggests that *Mox* has an ancestral role in mesoderm and possibly muscle formation in Bilateria. Expression of *Mox* during neurogenesis is evolved independently in arthropods and echinoderms. See main text for references. The simplified metazoan tree is adapted from figure 1a of Laumer et al., 2019.

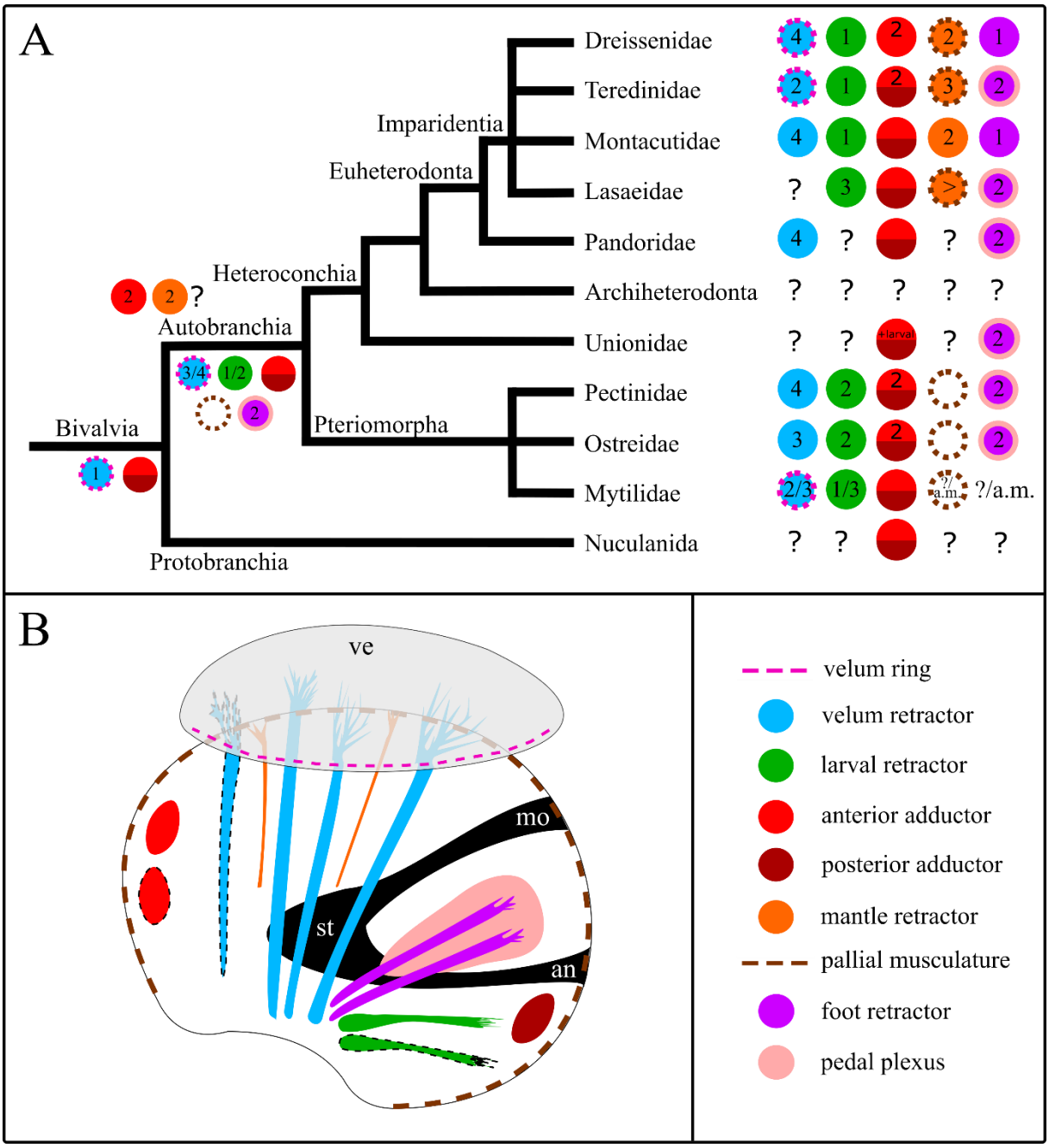


**Figure 14.** Muscle systems in bivalve lineages. A: Simplified Bivalvia tree (adapted from Combosch et al., 2017) represents the muscle systems in different taxa of bivalve larvae. ? (unknown), numbers (number of paired retractors/adductors), > (set of paired retractors), pink dotted outline of the blue point (prototroch/velum ring), brown dotted outline of the orange point or brown dotted circle (muscles of the pallial line), light pink outline of the purple point (pedal plexus), a.m. (after metamorphosis, note that is only marked for mytilids, while muscle systems of other bivalve larvae which are formed after metamorphosis are not noted). Colour

code indicates the other respective muscle systems. Comparative analysis implies that five muscle systems were present in the last common ancestor (LCA) of autobranch bivalve larvae, such as the velum musculature including three or four pairs of velum retractors and a velum muscle ring, the larval retractors (one or two pairs), the adductor system containing the anterior (might be paired) as well as the posterior adductor, the mantle musculature including the muscles of the pallial line and possibly two pairs of mantle retractors, and the foot musculature containing two pairs of foot retractors together with the pedal plexus. In addition, the data presently available suggest that the muscular ground pattern of bivalve larvae includes at least one pair of velum retractors, a velum muscle ring, the anterior and the posterior adductor. B: Schematic drawing of the muscle systems in the LCA of autobranch bivalve larva. See main text for references.

## Tables

**Table 1.** Species list for the gene annotation tree of the *myosin (II) heavy chain* gene (Figure 1) with associated NCBI/Ensembl Metazoa accession numbers. Most species are downloaded from the NCBI database, and a few are also retrieved from the Ensembl Metazoa database, which are marked with *. In addition, the *myosin II heavy chain* ortholog of *Acanthochitona crinita* is added from the transcriptome (De Oliveira et al., 2016), which is marked with X.

| **gene** | **species name (same in tree)** | **NCBI accession number / Ensembl Metazoa accession number *** |
|---|---|---|
| *myosin II heavy chain (mhc)* | *Dreissena rostriformis c1* | GHRL01011381 |
| *mhc* | *Dreissena rostriformis c2* | GHRL01034471 |
| *mhc* | *Dreissena rostriformis c3* | GHRL01017649 |
| *mhc* | *Dreissena rostriformis c4* | GHRL01006544 |
| *mhc* | *Acanthochitona crinita* | X |
| *mhc* | *Mytilus galloprovincialis* | CAB64662.1 |
| *mhc* | *Argopecten irradians* | AAC46490.1 |
| *mhc* | *Placopecten magellanicus* | AAB03661.1 |
| *mhc* | *Octopus bimaculoides* | CDG41623.1 |
| *mhc* | *Todarodes pacificus* | ADU19853.1 |
| *mhc* | *Onchidium struma* | AOR06339.1 |
| *mhc* | *Lingula anatine* | XP_023932278.1 |
| *mhc* | *Platynereis dumerilii* | AIJ28480.1 |
| *mhc* | *Drosophila melanogaster* | NP_523587.4 |
| *myosin I* | *Dreissena rostriformis c1* | GHRL01034922 |
| *myosin I* | *Dreissena rostriformis c2* | GHRL01003178 |
| *myosin I* | *Nematostella vectensis Ia* | * EDO49515 |
| *myosin I* | *Nematostella vectensis Ib* | * EDO45835 |
| *myosin I* | *Rattus norvegicus* | CAA50871.1 |
| *myosin I* | *Bos taurus* | AAA17565.1 |
| *myosin III* | *Dreissena rostriformis* | GHRL01023082 |
| *myosin III* | *Nematostella vectensis* | * EDO43631 |
| *myosin III* | *Anopheles darlingi* | ETN67236.1 |
| *myosin III* | *Athalia rosae* | XP_012256574.1 |
| *myosin III* | *Homo sapiens* | NP_059129.3 |
| *myosin V* | *Dreissena rostriformis* | GHRL01001522 |
| *myosin V* | *Nematostella vectensis* | * EDO41819 |
| *myosin V* | *Xenopus laevis* | AFU81219.2 |
| *myosin V* | *Drosophila melanogaster* | AAC99496.1 |
| *myosin V* | *Anopheles darlingi* | ETN63934.1 |
| *myosin VI* | *Dreissena rostriformis* | GHRL01023773 |

| | | |
|---|---|---|
| *myosin VI* | *Nematostella vectensis* | * EDO36037 |
| *myosin VI* | *Azumapecten farreri* | AAY63881.1 |
| *myosin VI* | *Crassostrea gigas* | * EKC25309.1 |
| *myosin VI* | *Anopheles darlingi* | ETN65262.1 |
| *myosin VI* | *Homo sapiens* | AAK00229.1 |
| *myosin VII* | *Dreissena rostriformis* | GHRL01032474 |
| *myosin VII* | *Nematostella vectensis* | * EDO45563 |
| *myosin VII* | *Crassostrea gigas* | * EKC28928.1 |
| *myosin VII* | *Leptochiton asellus* | ASM47588.1 |
| *myosin VII* | *Anopheles darlingi* | ETN66322.1 |
| *myosin VII* | *Homo sapiens* | AAB03679.1 |
| *myosin IX* | *Dreissena rostriformis* | GHRL01016224 |
| *myosin IX* | *Nematostella vectensis* | * EDO38834.1 |
| *myosin IX* | *Mizuhopecten yessoensis* | XP_021359286.1 |
| *myosin IX* | *Homo sapiens* | AAI40870.1 |
| *myosin XV* | *Dreissena rostriformis* | GHRL01005003 |
| *myosin XV* | *Crassostrea gigas* | * EKC41639.1 |
| *myosin XV* | *Cricetulus griseus* | EGW01271.1 |
| *myosin XV* | *Anopheles sinensis* | KFB48001.1 |
| *myosin XVIII* | *Dreissena rostriformis* | GHRL01021375 |
| *myosin XVIII* | *Crassostrea gigas* | * EKC35139.1 |
| *myosin XVIII* | *Pomacea canaliculate* | XP_025090257.1 |
| *myosin XVIII* | *Pan troglodytes* | JAA31795.1 |

**Table 2.** Species list for the single gene annotation tree of *even-skipped* and *Mox* genes (Figure 2) with associated NCBI accession numbers. All sequences are downloaded from the NCBI database. In addition, the orthologs of *even-skipped* and *Mox* of *Acanthochitona crinita* are added from the transcriptome (De Oliveira et al., 2016), which are marked with X.

| **gene** | **species name (same in tree)** | **NCBI accession number** |
|---|---|---|
| *even-skipped* | *Dreissena rostriformis* | GHRL01002417 |
| *even-skipped* | *Acanthochitona crinita* | X |
| *even-skipped* | *Alitta virens* | AOS87315.1 |
| *even-skipped* | *Membranipora membranacea* | ARJ36942.1 |
| *even-skipped* | *Nematostella vectensis* | SJX71987.1 |
| *even-skipped* | *Lineus ruber* | AMR72025.1 |
| *even-skipped* | *Owenia fusiformis* | AMY99557.1 |
| *even-skipped* | *Priapulus caudatus* | AKU77019.1 |
| *even-skipped* | *Terebratalia transversa* | AHY88463.1 |
| *Mox* | *Dreissena rostriformis c2* | GHRL01028895 |
| *Mox* | *Dreissena rostriformis c1* | GHRL01028894.1 |
| *Mox* | *Acanthochitona crinita* | X |
| *Mox* | *Alitta virens* | AOS87316.1 |
| *Mox* | *Haliotis rufescens* | CAA53027.1 |
| *Mox* | *Mizuhopecten yessoensis* | XP_021347798.1 |
| *Mox* | *Terebratalia transversa* | AJV21315.1 |
| *Mox* | *Mus musculus* | CAA78812.1 |
| *Hox1* | *Acanthochitona crinita* | APD15641.1 |
| *Hox1* | *Gymnomenia pellucida* | APD15663.1 |
| *Hox1* | *Nucula tumidula* | APD15698.1 |
| *Hox2* | *Acanthochitona crinita* | AKV16303.1 |
| *Hox2* | *Gymnomenia pellucida* | APD15664.1 |
| *Hox2* | *Nucula tumidula* | APD15699.1 |
| *Hox3* | *Acanthochitona crinita* | APD15643.1 |
| *Hox3* | *Nucula tumidula* | APD15700.1 |
| *Hox3* | *Wirenia argentea* | APD15711.1 |
| *Hox4* | *Dreissena rostriformis* | GHRL01028245 |
| *Hox4* | *Acanthochitona crinita* | APD15644.1 |
| *Hox4* | *Nucula tumidula* | APD15701.1 |
| *Hox4* | *Wirenia argentea* | APD15712.1 |
| *Hox5* | *Acanthochitona crinita* | APD15645.1 |
| *Hox5* | *Antalis entalis* | APD15655.1 |
| *Hox5* | *Gymnomenia pellucida* | APD15667.1 |

**Table 3.** Species list for the gene annotation tree of the *Brachyury* gene (Figure 3) with associated NCBI/Ensembl Metazoa accession numbers. Most sequences are downloaded from the NCBI database, and a few are also retrieved from the Ensembl Metazoa database, which are marked with *. In addition, the *Brachyury* ortholog of *Acanthochitona crinita* is added from the transcriptome (De Oliveira et al., 2016), which is marked with X.

| **gene** | **species name (same in tree)** | **NCBI accession number / Ensembl Metazoa accession number*** |
|---|---|---|
| *Brachyury* | *Dreissena rostriformis* | GHRL01029225 |
| *Brachyury* | *Acanthochitona crinita* | X |
| *Brachyury* | *Saccostrea kegaki* | BAG68616.1 |
| *Brachyury* | *Crassostrea gigas* | XP_011443609.1 |
| *Brachyury* | *Nematostella vectensis* | AAO27886.2 |
| *Brachyury* | *Patella vulgata* | CAD12821.1 |
| *Brachyury* | *Platynereis dumerilii* | CAC19335.1 |
| *Brachyury* | *Pomacea canaliculata* | XP_025098368.1 |
| *Brachyury* | *Tribolium castaneum* | NP_001034532.1 |
| *Brachyury* | *Lingula anatina* | XP_013385442.1 |
| *Eomes* | *Dreissena rostriformis* | GHRL01021264 |
| *Eomes* | *Cervus elaphus hippelaphus* | OWK02840.1 |
| *Eomes* | *Danio rerio* | NP_571754.3 |
| *Eomes* | *Xenopus tropicalis* | AAI67292.1 |
| *Tbx1* | *Nematostella vectensis* | AAQ23383.1 |
| *Tbx1* | *Crassostrea gigas* | XP_011442237.1 |
| *Tbx1* | *Mizuhopecten yessoensis* | OWF41599.1 |
| *Tbx2* | *Dreissena rostriformis* | GHRL01022900 |
| *Tbx2* | *Culex quinquefasciatus* | EDS41352.1 |
| *Tbx2* | *Crassostrea gigas* | * EKC26468.1 |
| *Tbx2* | *Mizuhopecten yessoensis* | XP_021365993.1 |
| *Tbx2* | *Lingula anatina* | XP_013379452.1 |
| *Tbx3* | *Dreissena rostriformis* | GHRL01036745.1 |
| *Tbx3* | *Lingula anatina* | XP_013379419.1 |
| *Tbx3* | *Biomphalaria glabrata* | XP_013085613.1 |
| *Tbx3* | *Crassostrea gigas* | XP_011436735.1 |
| *Tbx4* | *Cervus elaphus hippelaphus* | OWK13929.1 |
| *Tbx4* | *Larimichthys crocea* | XP_019124927.1 |
| *Tbx4* | *Tachysurus fulvidraco* | XP_027003995.1 |
| *Tbx5* | *Danio rerio* | AAF06733.1 |
| *Tbx5* | *Struthio camelus* | AIA82401.1 |
| *Tbx5* | *Cervus elaphus hippelaphus* | OWK14983.1 |
| *Tbx6* | *Danio rerio* | NP_705952.2 |
| *Tbx6* | *Xenopus laevis* | BAC20262.1 |
| *Tbx6* | *Mus musculus* | AAT72924.1 |

| | | |
|---|---|---|
| *Tbx8* | *Toxocara canis* | KHN81917.1 |
| *Tbx8* | *Caenorhabditis elegans* | BAD14918.1 |
| *Tbx8* | *Pristionchus pacificus* | PDM70138.1 |
| *Tbx15* | *Dreissena rostriformis* | GHRL01011340.1 |
| *Tbx15* | *Mizuhopecten yessoensis* | OWF43000.1 |
| *Tbx15* | *Crassostrea gigas* | * EKC21660.1 |
| *Tbx15* | *Rattus norvegicus* | NP_001099921.1 |
| *Tbx15* | *Nestor notabilis* | KFQ43989.1 |
| *Tbx20* | *Dreissena rostriformis c1* | GHRL01025755 |
| *Tbx20* | *Dreissena rostriformis c2* | GHRL01025754 |
| *Tbx20* | *Mizuhopecten yessoensis* | OWF44695.1 |
| *Tbx20* | *Crassostrea gigas* | * EKC38760.1 |
| *Tbx20* | *Lingula anatina* | XP_013390981.1 |
| *Tbx20* | *Exaiptasia pallida* | KXJ24557.1 |
| *Tbx20* | *Cricetulus griseus* | RLQ68618.1 |

**Table 4.** Annotated genes of interest (*Brachyury*, *even-skipped*, *Mox_c2*, *myosin II heavy chain_c1*) of *Dreissena rostriformis* for *in situ* hybridization with corresponding forward- and reverse- primers and insert length. (bp: base pair).

| **gene of interest** | **forward primer** | **reverse primer** | **insert length** |
|---|---|---|---|
| *Brachyury* | CCAAGTTCAAGGAATACACC | GCACGAAACTAGAGATGTC | 1037 bp |
| *even-skipped* | GATATGTATGAGGACGAC | GTGGAGTATTTATCGACTG | 849 bp |
| *Mox_c2* | GATCATAATCAGATGTACGGG | CCGACGAATAATCATCAC | 891 bp |
| *myosin II heavy chain_c1* | GATCCAGAGAAACATCAGG | GACTCATGCTGCATGGTC | 1122 bp |

**Table 5.** Relative expression values of genes of interest in different stages (hours post fertilization - hpf) of *Dreissena rostriformis* corresponding to those in Figure 4. Highest values per gene are marked in yellow.

| | ***Brachyury*** | ***even-skipped*** | ***Mox_c1*** | ***Mox_c2*** | ***mhc_c1*** | ***mhc_c2*** | ***mhc_c3*** | ***mhc_c4*** |
|---|---|---|---|---|---|---|---|---|
| **0 hpf** | 0,00 | 0,00 | 0,00 | 0,00 | 0,85 | 0,06 | 0,30 | 17,46 |
| **2 hpf** | 0,00 | 0,00 | 0,00 | 0,00 | 1,18 | 0,02 | 0,72 | 31,04 |
| **4 hpf** | 4,90 | 5,84 | 0,00 | 0,16 | 0,91 | 0,11 | 1,08 | 27,11 |
| **6 hpf** | 3,09 | 1,93 | 0,00 | 0,00 | 1,97 | 0,30 | 1,44 | 24,60 |
| **8 hpf** | 133,43 | 24,36 | 0,00 | 0,00 | 2,03 | 0,43 | 4,23 | 15,67 |
| **13 hpf** | 179,17 | 275,63 | 0,00 | 0,20 | 8,26 | 0,89 | 25,53 | 9,90 |
| **18 hpf** | 92,97 | 149,70 | 0,00 | 0,20 | 15,36 | 0,42 | 62,54 | 22,93 |
| **23 hpf** | 59,27 | 48,39 | 0,16 | 2,49 | 8,65 | 4,28 | 88,26 | 25,38 |
| **26 hpf** | 61,57 | 57,15 | 0,00 | 12,95 | 11,53 | 17,97 | 209,04 | 28,06 |
| **27 hpf** | 65,40 | 30,59 | 0,16 | 4,89 | 44,65 | 41,57 | 221,31 | 33,27 |
| **30 hpf** | 47,61 | 16,77 | 0,00 | 1,17 | 43,08 | 26,49 | 149,64 | 40,49 |
| **36 hpf** | 72,74 | 32,86 | 1,64 | 18,93 | 218,16 | 43,88 | 810,44 | 66,85 |
| **48 hpf** | 50,31 | 10,02 | 0,11 | 4,60 | 93,24 | 14,39 | 260,52 | 65,71 |
| **54 hpf** | 48,16 | 10,18 | 0,11 | 4,73 | 59,65 | 12,77 | 219,20 | 71,51 |
| **60 hpf** | 54,98 | 22,21 | 2,91 | 6,99 | 209,68 | 22,68 | 761,55 | 79,14 |
| **72 hpf** | 66,37 | 23,90 | 3,46 | 3,90 | 213,05 | 26,08 | 734,96 | 57,61 |
| **84 hpf** | 62,13 | 20,33 | 2,70 | 7,27 | 171,93 | 20,08 | 591,15 | 49,18 |

**Table 6.** Annotated genes of *Dreissena rostriformis* used for *in situ* hybridization and phylogenetic analysis containing domains by using Pfam and NCBI accession numbers.

| **annotated gene** | **domains** | **NCBI accession number** |
|---|---|---|
| *Dreissena_rostriformis_Brachyury* | T-box | GHRL01029225 |
| *Dreissena_rostriformis_Eomes* | fragmented T-box | GHRL01021264 |
| *Dreissena_rostriformis_Tbx2* | T-box | GHRL01022900 |
| *Dreissena_rostriformis_Tbx3* | T-box | GHRL01036745.1 |
| *Dreissena_rostriformis_Tbx15* | T-box | GHRL01011340.1 |
| *Dreissena_rostriformis_c1_Tbx20* | T-box | GHRL01025755 |
| *Dreissena_rostriformis_c2_Tbx20* | T-box | GHRL01025754 |
| *Dreissena_rostriformis_even-skipped* | homeodomain | GHRL01002417 |
| *Dreissena_rostriformis_c1_Mox* | homeodomain | GHRL01028894.1 |
| *Dreissena_rostriformis_c2_Mox* | homeodomain | GHRL01028895 |
| *Dreissena_rostriformis_Hox4* | homeodomain | GHRL01028245 |
| *Dreissena_rostriformis_c1_myosin_I* | fragmented myosin head, myosin TH1 | GHRL01034922 |
| *Dreissena_rostriformis_c2_myosin_I* | fragmented myosin head, 2x IQ | GHRL01003178 |
| *Dreissena_rostriformis_c1_myosin_II_heavy_chain* | myosin N, myosin head, myosin tail 1 | GHRL01011381 |
| *Dreissena_rostriformis_c2_myosin_II_heavy_chain* | myosin N, myosin head, IQ, myosin tail 1 | GHRL01034471 |
| *Dreissena_rostriformis_c3_myosin_II_heavy_chain* | myosin N, myosin head, myosin tail 1 | GHRL01017649 |
| *Dreissena_rostriformis_c4_myosin_II_heavy_chain* | fragmented myosin head, myosin tail 1, myosin tail 1 | GHRL01006544 |
| *Dreissena_rostriformis_myosin_III* | Pkinase, myosin head, 5x IQ | GHRL01023082 |
| *Dreissena_rostriformis_myosin_V* | fragmented myosin head | GHRL01001522 |
| *Dreissena_rostriformis_myosin_VI* | myosin N, fragmented myosin head, myosin VI – CBD | GHRL01023773 |
| *Dreissena_rostriformis_myosin_VII* | myosin head, 3x IQ | GHRL01032474 |
| *Dreissena_rostriformis_myosin_IX* | 3x fragmented myosin head, 3x IQ, fragmented RhoGAP | GHRL01016224 |
| *Dreissena_rostriformis_myosin_XV* | 3x fragmented myosin head, MyTH4 | GHRL01005003 |
| *Dreissena_rostriformis_myosin_XVIII* | fragmented myosin head | GHRL01021375 |

**References**


Abascal, F.; Zardoya, R.; Posada, D. ProtTest: selection of best-fit models of protein evolution. Bioinformatics **2005**, 21, 9, 2104-2105.

Ahringer, J. Posterior patterning by the *Caenorhabditis elegans even-skipped* homolog *vab-7*. Genes & Development **1996**, 10, 1120-1130.

Altnöder, A.; Haszprunar, G. Larval Morphology of the Brooding Clam *Lasaea adansonii* (Gmelin, 1791) (Bivalvia, Heterodonta, Galeommatoidea). Journal of Morphology **2008**, 269, 762-774.

Altschul, S.F.; Gish, W.; Miller, W.; Myers, E.W.; Lipman, D.J. Basic Local Alignment Search Tool. Journal of Molecular Biology **1990**, 215, 3, 403-410.

Andrikou, C.; Iovene, E.; Rizzo, F.; Oliveri, P.; Arnone, M.I. Myogenesis in the sea urchin embryo: the molecular fingerprint of the myoblast precursor. EvoDevo **2013**, 4, 33.

Andrikou, C.; Arnone, M.I. Too many ways to make a muscle: Evolution of GRNs governing myogenesis. Zoologischer Anzeiger **2015**, 256, 2-13.

Andrikou, C.; Passamaneck, Y.J.; Lowe, C.J.; Martindale, M.Q.; Hejnol, A. Molecular patterning during the development of *Phoronopsis harmeri* reveals similarities to rhynchonelliform brachiopods. EvoDevo **2019**, 10, 13.

Andrikou, C.; Hejnol, A. FGF signaling induces mesoderm in members of Spiralia. bioRxiv **2020**, doi: 10.1101/2020.08.13.249714.

Audino, J.A.; Marian, J.E.A.R.; Kristof, A.; Wanninger, A. Inferring muscular ground patterns in Bivalvia: Myogenesis in the scallop *Nodipecten nodosus*. Frontiers in Zoology **2015**, 12, 34.

Bassham, S.; Postlethwait, J. *Brachyury* (*T*) Expression in Embryos of a Larvacean Urochordate, *Oikopleura dioica*, and the Ancestral Role of *T*. Developmental Biology **2000**, 220, 322-332.

Burgess, D.R. Cytokinesis: New Roles for Myosin. Current Biology **2005**, 15, 8, R310-R311.

Candia, A.F.; Hu, J.; Crosby, J.; Lalley, P.A.; Noden, D.; Nadeau, J.H.; Wright, C.V.E. *Mox-1* and *Mox-2* define a novel homeobox gene subfamily and are differentially expressed during early mesodermal patterning in mouse embryos. Development **1992**, 116, 1123-1136.

Candia, A.F.; Wright, C.V.E. The expression pattern of *Xenopus Mox-2* implies a role in initial mesodermal differentiation. Mechanisms of Development **1995**, 52, 27-36.

Candia, A.F.; Wright, C.V.E. Differential localization of Mox-1 and Mox-2 proteins indicates distinct roles during development. The International Journal of Developmental Biology **1996**, 40, 6, 1179-1184.

Calcino, A.D.; De Oliveira, A.L.; Simakov, O.; Schwaha, T.; Zieger, E.; Wollesen, T.; Wanninger, A. The quagga mussel genome and the evolution of freshwater tolerance. DNA Research **2019**, 26, 5, 411-422.

Chiang, C.; Patel, N.H.; Young, K.E.; Beachy, P.A. The novel homeodomain gene *buttonless* specifies differentiation and axonal guidance functions of *Drosophila* dorsal median cells. Development **1994**, 120, 3581-3593.

Chiodin, M.; Børve, A.; Berezikov, E.; Ladurner, P.; Martinez, P.; Hejnol, A. Mesodermal Gene Expression in the Acoel *Isodiametra pulchra* Indicates a Low Number of Mesodermal Cell Types and the Endomesodermal Origin of the Gonads. PLoS ONE **2013**, 8, e55499.

Chiori, R.; Jager, M.; Denker, E.; Wincker, P.; Da Silva, C.; Le Guyader, H.; Manuel, M.; Quéinnec, E. Are Hox Genes Ancestrally Involved in Axial Patterning? Evidence from the Hydrozoan *Clytia hemisphaerica* (Cnidaria). PLoS ONE **2009**, 4, 1, e4231.

Conlon, F.L.; Fairclough, L.; Price, B.M.J.; Casey, E.S.; Smith, J.C. Determinants of T-box protein specifity. Development **2001**, 128, 3749-3758.

Copf, T.; Rabet, N.; Celniker, S.E.; Averof, M. Posterior patterning genes and the identification of unique body region in the brine shrimp *Artemia franciscana.* Development **2003**, 130, 5915-5927.

Cragg, S.M. The adductor and retractor muscles of the veliger of *Pecten maximus* (L.) (Bivalvia). Journal of Molluscan Studies **1985**, 51, 276-283.

Cragg, S.M. Biology and Ecology of Scallop Larvae. In Scallops – Biology, Ecology, Aquaculture, and Fisheries; Shumway, S.E., Parsons, G.J., Eds,; Elsevier: Amsterdam, **2016**, 40; pp. 31-73 ISBN 9780444627100.

Criscuolo, A.; Gribaldo, S. BMGE (Block Mapping and Gathering with Entropy): a new software for selection of phylogenetic informative regions from multiple sequence alignments. BMC Evolutionary Biology **2010**, 10, 210.

Damen, W.G.M.; Weller, M.; Tautz, D. Expression patterns of *hairy*, *even-skipped*, and *runt* in the spider *Cupiennius salei* imply that these genes were segmentation genes in a basal arthropod. PNAS **2000**, 97, 9, 4515-4519.

De Oliveira, A.L.; Wollesen, T.; Kristof, A.; Scherholz, M.; Redl, E.; Todt, C.; Bleidorn, C.; Wanninger, A. Comparative transcriptomics enlarges the toolkit of known developmental genes in mollusks. BMC Genomics **2016**, 17, 905.

De Ventura, L.; Kopp, K.; Seppälä, K.; Jokela, J. Tracing the quagga mussel invasion along the Rhine river system using eDNA markers: early detection and surveillance of invasive zebra and quagga mussels. Management of Biological Invasions **2017**, 8, 1, 101-112.

Drew, G.A. Some observations on the habits, anatomy and embryology of members of the Protobranchia. Anatomischer Anzeiger **1899**, 15, 493-519.

Drew, G.A. The life history of *Nucula delphinodonta* (Mighels). The Quarterly Journal of Microscopical Science **1901**, 44, 313-391.

Dyachuk, V.; Odintsova, N. Development of the larval muscle system in the mussel *Mytilus trossulus* (Mollusca, Bivalvia). Development Growth and Differentiation **2009**, 51, 69-79.

Erkenbrack, E.M. Divergence of ectodermal and mesodermal gene regulatory network lineages in early development of sea urchins. PNAS **2016**, 113, 46, E7202-E7211.

Ferrier, D.E.K.; Minguillón, C.; Cebrián, C.; Garcia-Fernàndez, J. Amphioxus Evx Genes: Implications for the Evolution of the Midbrain-Hindbrain Boundary and the Chordate Tailbud. Developmental Biology **2001**, 237, 270-281.

Foth, B.J.; Goedecke, M.C.; Soldati, D. New insights into myosin evolution and classification. PNAS **2006**, 103, 10, 3681-3686.

Fujioka, M.; Wessells, R.J.; Han, Z.; Liu, J.; Fitzgerald, K.; Yusibova, G.L.; Zamora, M.; Ruiz-Lozano, P.; Bodmer, R.; Jaynes, J.B. Embryonic *even-skipped*-Dependent Muscle and Heart Cell Fates Are Required for Normal Adult Activity, Heart Function, and Lifespan. Circulation Research **2005**, 97, 1108-1114.

Furlong, E.E.M.; Andersen, E.C.; Null, B.; White, K.P.; Scott, M.P. Patterns of Gene Expression During Drosophila Mesoderm Development. Science **2001**, 293, 1629-1633.

Giribet, G. Bivalvia. In Phylogeny and Evolution of the Mollusca; Ponder, W.F., Lindberg, D.R., Eds.; University of California Press: Berkeley, Los Angeles, London, **2008**, 6; pp. 105-141 ISBN 9780520250925.

Green, J.E.; Akam, M. Germ cells of the centipede *Strigamia maritima* are specified early in embryonic development. Developmental Biology **2014**, 392, 419-430.

Guindon, S.; Gascuel, O. A Simple, Fast, and Accurate Algorithm to Estimate Large Phylogenies by Maximum Likelihood. Systematic Biology **2003**, 52, 5, 696-704.

Hebers, K. Entwicklungsgeschichte von *Anodonta cellensis* Schröt. Zeitschrift für wissenschaftliche Zoologie **1913**, 108, 1-174.

Hérault, Y.; Hraba-Renevey, S.; van der Hoeven, F.; Duboule, D. Function of the *Evx-2* gene in the morphogenesis of vertebrate limbs. The EMBO Journal **1996**, 15, 23, 6727-6738.

Hejnol, A.; Martindale, M.Q. Acoel development indicates the independent evolution of the bilaterian mouth and anus. Nature **2008a**, 456, 382-386.

Hejnol, A.; Martindale, M.Q. Acoel development supports a simple planula-like urbilaterian. Philosophical Transactions of the Royal Society B **2008b**, 363, 1493-1501.

Hejnol, A.; Martín-Durán, J.M. Getting to the bottom of anal evolution. Zoologischer Anzeiger **2015**, 256, 61-74.

Hinman, V.F.; Degnan B.M. *Mox* homeobox expression in muscle lineage of the gastropod *Haliotis asinina*: evidence for a conserved role in bilaterian myogenesis. Development Genes and Evolution **2002**, 212, 141-144.

Howe, K.L; Contreras-Moreira, B.; De Silva, N.; Maslen, G.; Akanni, W.; Allen, J.; Alvarez-Jarreta, J.; Barba, M.; Bolser, D.M.; Cambell, L.; Carbajo, M.; Chakiachvili, M.; Christensen, M.; Cummins, C.; Cuzick, A.; Davis, P.; Fexova, S.; Gall, A.; George, N.; Gil, L.; Gupta, P.; Hammond-Kosack, K.E.; Haskell, E.; Hunt, S.E.; Jaiswal, P.; Janacek, S.H.; Kersey, P.J.; Langridge, N.; Maheswari, U.; Maurel, T.; McDowall, M.D.; Moore, B.; Muffato, M.; Naamati, G.; Naithani, S.; Olson, A.; Papatheodorou, I.; Patricio, M.; Paulini, M.; Pedro, H.; Perry, E.; Preece, J.; Rosello, M.; Russell, M.; Sitnik, V.; Staines, D.M.; Stein, J.; Tello-Ruiz, M.K.; Trevanion, S.J.; Urban, M.; Wei, S.; Ware, D.; Williams, G.; Yates, A.D.; Flicek, P. Ensembl Genomes 2020—enabling non-vertebrate genomic research. Nucleic Acids Research **2020**, 48, D689-D695.

Ikuta, T.; Yoshida, N.; Satoh, N.; Saiga, H. *Ciona intestinalis* Hox gene cluster: Its dispersed structure and residual colinear expression in development. PNAS **2004**, 101, 42, 15118-15123.

Janssen, R.; Budd, G.E.; Prpic, N.M.; Damen. W.G.M. Expression of myriapod pair rule gene orthologs. EvoDevo **2011**, 2, 5.

Jones, D.T.; Taylor, W.R.; Thornton, J.M. The rapid generation of mutation data matrices from protein sequences. Bioinformatics **1992**, 8, 3, 275-282.

Kakoi, S.; Kin, K.; Miyazaki, K.; Wada, H. Early Development of the Japanese Spiny Oyster (*Saccostrea kegaki*): Characterization of Some Genetic Markers. Zoological Science **2008**, 25, 455-464.

Katoh, K.; Misawa, K.; Kuma, K.; Miyata, T. MAFFT: a novel method for rapid multiple sequence alignment based on fast Fourier transform. Nucleic Acids Research **2002**, 30, 14, 3059-3066.

Kin, K.; Kakoi, S.; Wada, H. A novel role for *dpp* in the shaping of bivalve shells revealed in a conserved molluscan developmental program. Developmental Biology **2009**, 329, 152-166.

Kobayashi, C.; Kobayashi, S.; Orii, H.; Watanabe, K.; Agata, K. Identification of Two Distinct Muscles in the Planarian *Dugesia japonica* by their Expression of Myosin Heavy Chain Genes. Zoological Science **1998**, 15, 861-869.

Koop, D.; Richards, G.S.; Wanninger, A.; Gunter, H.M.; Degnan, B.M. The role of MAPK signaling in patterning and establishing axial symmetry in the gastropod *Haliotis asinina*. Developmental Biology **2007**, 311, 200-212.

Kozin, V.V.; Filimonova, D.A.; Kupriashova, E.E.; Kostyuchenko, R.P. Mesoderm patterning and morphogenesis in the polychaete *Alitta virens* (Spiralia, Annelida): Expression of mesodermal markers *Twist*, *Mox*, *Evx* and functional role for MAP kinase signaling. Mechanisms of Development **2016**, 140, 1-11.

Kurita, Y.; Hashimoto, N.; Wada, H. Evolution of the molluscan body plan: the case of the anterior adductor muscle of bivalves. Biological Journal of the Linnean Society **2016**, 119, 420-429.

Kusch, T.; Reuter., R. Functions for *Drosophila brachyenteron* and *forkhead* in mesoderm specification and cell signalling. Development **1999**, 126, 3991-4003.

Larsson, A. AliView: a fast and lightweight alignment viewer and editor for large datasets. Bioinformatics **2014**, 30, 22, 3276-3278.

Lartillot, N.; Lespinet, O.; Vervoort, M.; Adoutte, A. Expression pattern of *Brachyury* in the mollusc *Patella vulgata* suggests a conserved role in the establishment of the AP axis in Bilateria. Development **2002**, 129, 1411-1421.

Laumer, C.E.; Fernández, R.; Lemer, S.; Combosch, D.; Kocot, K.M.; Riesgo, A.; Andrade, S.C.S.; Sterrer, W.; Sørensen, M.V.; Giribet, G. Revisiting metazoan phylogeny with genomic sampling of all phyla. Proceedings of the Royal Society B: Biological Sciences **2019**, 286, 20190831.

Le, S.Q.; Gascuel, O. An Improved General Amino Acid Replacement Matrix. Molecular Biology and Evolution **2008**, 25, 7, 1307-1320.

Leininger, S.; Adamski, M.; Bergum, B.; Guder, C.; Liu, J.; Laplante, M.; Bråte, J.; Hoffmann, F.; Fortunato, S.; Jordal, S.; Rapp, H.T.; Adamska, M. Developmental gene expression provides clues to relationships between sponge and eumetazoan body plans. Nature communications **2014**, 5, 3905.

Li, E.; Cui, M.; Peter, I.S.; Davidson, E.H. Encoding regulatory state boundaries in the pregastrular oral ectoderm of the sea urchin embryo. PNAS **2014**, 111, 10, E906-E913.

Li, H.; Li, Q.; Yu, H.; Du, S. Developmental dynamics of myogenesis in Pacific oyster *Crassostrea gigas*. Comparative Biochemistry and Physiology, Part B, **2019**, 227, 21-30.

Lowe, C.J.; Terasaki, M.; Wu, M.; Freeman, Jr. R.M.; Runft, L.; Kwan, K.; Haigo, S.; Aronowicz, J.; Lander, E.; Gruber, C.; Smith, M.; Kirschner, M.; Gerhart, J. Dorsoventral Patterning in Hemichordates: Insights into Early Chordate Evolution. PLoS Biology **2006**, 4, 9, e291, 1603-1619.

Mankoo, B.S.; Collins, N.S.; Ashby, P.; Grigorieva, E.; Pevny, L.H.; Candia, A.; Wright, C.V.E.; Rigby, P.W.J., Pachnis, V. *Mox2* is a component of the genetic hierarchy controlling limb muscle development. Nature **1999**, 400, 69-73.

Martín-Durán, J.M.; Romero, R. Evolutionary implications of morphogenesis and molecular patterning of the blind gut in the planarian *Schmidtea polychroa*. Developmental Biology **2011**, 352, 164-176.

Martín-Durán, J.M.; Janssen, R.; Wennberg, S.; Budd, G.E.; Hejnol, A. Deuterostomic Development in the Protostome *Priapulus caudatus*. Current Biology **2012**, 22, 2161-2166.

Martín-Durán, J.M.; Hejnol, A. The study of *Priapulus caudatus* reveals conserved molecular patterning underlying different gut morphogenesis in the Ecdysozoa. BMC Biology **2015**, 13, 29.

Martín-Durán, J.M.; Vellutini, B.C.; Hejnol, A. Evolution and development of the adelphophagic, intracapsular Schmidt´s larva of the nemertean *Lineus ruber*. EvoDevo **2015**, 6, 28.

Martín-Durán, J.M.; Passamaneck, Y.J.; Martindale, M.Q.; Hejnol, A. The developmental basis for the recurrent evolution of deuterostomy and protostomy. Nature Ecology & Evolution **2016**, 1, 0005.

Minguillón, C.; Garcia-Fernàndez, J. The Single Amphioxus Mox Gene: Insights into the Functional Evolution of Mox Genes, Somites, and the Asymmetry of Amphioxus Somitogenesis. Developmental Biology **2002**, 246, 455-465.

Minguillón, C.; Garcia-Fernàndez, J. Genesis and evolution of the *Evx* and *Mox* genes and the extended Hox and ParaHox gene clusters. Genome Biology **2003**, 4, 2, R12.

Neyt, C.; Jagla, K.; Thisse, C.; Thisse, B.; Haines, L.; Currie, P.D. Evolutionary origins of vertebrate appendicular muscle. Nature **2000**, 408, 82-86.

Nishino, A.; Satou, Y.; Morisawa, M.; Satoh, N. *Brachyury (T)* gene expression and notochord development in *Oikopleura longicauda* (Appendicularia, Urochordata). Development Genes and Evolution **2001**, 211, 219-231.

Patel, N.H.; Ball, E.E.; Goodman, C.S. Changing role of *even-skipped* during the evolution of insect pattern formation. Nature **1992**, 357, 339-342.

Patel, N.H.; Condron, B.G.; Zinn, K. Pair-rule expression patterns of *even-skipped* are found in both short- and long-germ beetles. Nature **1994**, 367, 429-434.

Passamaneck, Y.J.; Hejnol, A.; Martindale, M.Q. Mesodermal gene expression during the embryonic and larval development of the articulate brachiopod *Terebratalia transversa*. EvoDevo **2015**, 6, 10.

Perry, K.J.; Lyons, D.C.; Truchado-Garcia, M.; Fischer, A.H.L.; Helfrich, L.W.; Johansson, K.B.; Diamond, J.C.; Grande, C.; Henry, J.Q. Deployment of Regulatory Genes During Gastrulation and Germ Layer Specification in a Model Spiralian Mollusc *Crepidula*. Developmental Dynamics **2015**, 244, 1215-1248.

Peter, I.S.; Davidson, E.H. A gene regulatory network controlling the embryonic specification of endoderm. Nature **2011**, 474, 635-639.

Peterson, K.J.; Cameron, R.A.; Tagawa, K.; Satoh, N.; Davidson, E.H. A comparative molecular approach to mesodermal patterning in basal deuterostomes: the expression pattern of *Brachyury* in the enteropneust hemichordate *Ptychodera flava*. Development **1999**, 126, 85-95.

Pocock, R.; Ahringer, J.; Mitsch, M.; Maxwell, S.; Woollard, A. A regulatory network of T-box genes and the *even-skipped* homologue *vab-7* controls patterning and morphogenesis in *C. elegans*. Development **2004**, 131, 2373-2385.

Poustka, A.J.; Kühn, A.; Groth, D.; Weise, V.; Yaguchi, S.; Burke, R.D.; Herwig, R.; Lehrach, H.; Panopoulou, G. A global view of gene expression in lithium and zinc treated sea urchin embryos: new components of gene regulatory networks. Genome Biology **2007**, 8, 5, R85.

Rallis, C.; Stamataki, D.; Pontikakis, S.; Mankoo, B.S.; Karagogeos, D. Isolation of the avian homologue of the homeobox gene *Mox2* and analysis of its expression pattern in developing somites and limbs. Mechanisms of Development **2001**, 104, 121-124.

Renfer, E.; Amon-Hassenzahl, A.; Steinmetz, P.R.H.; Technau, U. A muscle-specific transgenic reporter line of the sea anemone, *Nematostella vectensis*. PNAS **2010**, 107, 1, 104-108.

Rieger, R.; Haszprunar, G.; Hobmayer, B. Bilateria. In Spezielle Zoologie, Teil 1: Einzeller und Wirbellose Tiere; Westheide, W., Rieger, G., Eds.; Springer: Berlin, Heidelberg, **2013**, 3; pp. 293-356 ISBN 9783642346958.

Ruiz i Altaba, A.; Melton, D.A. Involvement of the Xenopus Homeobox Gene Xhox3 in Pattern Formation along the Anterior-Posterior Axis. Cell **1989**, 57, 317-326.

Ruvkun, G.; Hobert, O. The Taxonomy of Developmental Control in *Caenorhabditis elegans*. Science **1998**, 282, 2033-2041.

Ryan, J.F.; Mazza, M.E.; Pang, K.; Matus, D.Q.; Baxevanis, A.D.; Martindale, M.Q.; Finnerty, J.R. Pre-Bilaterian Origins of the Hox Cluster and the Hox Code: Evidence from the Sea Anemone, *Nematostella vectensis*. PLoS ONE **2007**, 2, e153, 1-23.

Ryan, J.F.; Pang, K.; NISC Comparative Sequencing Program; Mullikin, J.C.; Martindale, M.Q.; Baxevanis, A.D. The homeodomain complement of the ctenophore *Mnemiopsis leidyi* suggests that Ctenophora and Porifera diverged prior to the ParaHoxozoa. EvoDevo **2010**, 1, 9.

Satou, Y.; Imai, K.S. Gene regulatory systems that control gene expression in the *Ciona* embryo. Proceedings of the Japan Academy, Series B, Physical and biological sciences **2015**, 91, 2, 33-50.

Salvini-Plawen, L.v.; Haszprunar, G. Mollusca, Weichtiere. In Spezielle Zoologie, Teil 1: Einzeller und Wirbellose Tiere; Westheide, W., Rieger, G., Eds.; Springer: Berlin, Heidelberg, **2013**, 3; pp. 293-356 ISBN 9783642346958.

Schierwater, B.; Kamm, K.; Srivastava, M.; Rokhsar, D.; Rosengarten, R.D.; Dellaporta, S.L. The Early ANTP Gene Repertoire: Insights from the Placozoan Genome. PLoS ONE **2008**, 3, e2457.

Sebé-Pedrós, A.; Ariza-Cosano, A.; Weirauch, M.T.; Leininger, S.; Yang, A.; Torruella, G.; Adamski, M.; Adamska, M.; Hughes, T.R.; Gómez-Skarmeta, J.L.; Ruiz-Trillo, I. Early evolution of the T-box transcription factor family. PNAS **2013**, 110, 40, 16050-16055.

Sebé-Pedrós, A.; Ruiz-Trillo, I. Evolution and Classification of the T-Box Transcription Factor Family. In T-box Genes in Development and Disease; Frasch, M., Ed.; Elsevier, Academic Press, Current Topics in Developmental Biology **2017**, 122; pp. 1-26 ISBN 9780128013809.

Seebald, J.L.; Szeto, D.P. Zebrafish *eve1* regulates the lateral and ventral fates of mesodermal progenitor cells at the onset of gastrulation. Developmental Biology **2011**, 349, 78-89.

Sordino, P.; Duboule, D.; Kondo, T. Zebrafish *Hoxa* and *Evx-2* genes: cloning, developmental expression and implications for the functional evolution of posterior *Hox* genes. Mechanisms of Development **1996**, 59, 165-175.

Sun, X.; Liu, Z.; Zhou, L.; Wu, B.; Yang, A.; Tian, J. Developmental Dynamics of the Larval Muscle System of Bay Scallop (*Agropecten irradians*). Journal of Ocean University of China **2020**, 19, 386-392.

Sun, X.; Zheng, Y.; Yu, T.; Wu, B.; Liu, Z.; Zhou, L.; Tian, J.; Yang, A. Developmental dynamics of myogenesis in Yesso Scallop *Patinopecten yessoensis*. Comparative Biochemistry and Physiology, Part B **2019**, 228, 51-60.

Takada, N.; Goto, T.; Sato, N. Expression Pattern of the *Brachyury* Gene in the Arrow Worm *Paraspadella gotoi* (Chaetognatha). Genesis **2002**, 32, 240-245.

Tan, S.; Huan, P.; Liu, B. Expression patterns indicate that BMP2/4 and Chordin, not BMP5-8 and Gremlin, mediate dorsal-ventral patterning in the mollusk *Crassostrea gigas*. Development Genes and Evolution **2017**, 227, 75-84.

Terazawa, K.; Satoh, N. Formation of the chordamesoderm in the amphioxus embryo: Analysis with *Brachyury* and *fork head/HNF-3* genes. Development Genes and Evolution **1997**, 207, 1-11.

Thompson, R.F.; Langford, G.M. Myosin Superfamily Evolutionary History. The Anatomical Record **2002**, 268, 276-289.

Vellutini, B.C.; Martín-Durán, J.M.; Hejnol, A. Cleavage modification did not alter early blastomere fates during bryozoan evolution. BMC Biology **2017**, 15, 33.

Wanninger, A.; Wollesen, T. Mollusca. In Evolutionary Developmental Biology of Invertebrates; Wanninger, A., Ed.; Springer: Vienna, **2015**, 2; pp. 103-153 ISBN 9783709118719.

Waterhouse, A.M.; Procter, J.B.; Martin, D.M.A.; Clamp, M.; Barton, G.J. Jalview Version 2—a multiple sequence alignment editor and analyses workbench. Bioinformatics **2009**, 25, 9, 1189-1191.

Wurzinger-Mayer, A.; Shipway, J.R.; Kristof, A.; Schwaha, T.; Cragg, S.M.; Wanninger, A. Developmental dynamics of myogenesis in the shipworm *Lyrodus pedicellatus* (Mollusca: Bivalvia). Frontiers in Zoology **2014**, 11, 90.

Yamada, A.; Pang, K.; Martindale, M.Q.; Tochinai, S. Surprisingly complex T-box gene complement in diploblastic metazoans. Evolution & Development **2007**, 9, 3, 220-230.

Zhang, S.; Bernstein, S.I. Spatially and temporally regulated expression of myosin heavy chain alternative exons during *Drosophila* embryogenesis. Mechanisms of Development **2001**, 101, 35-45.

**Zusammenfassung**

Für alle Bilateria ist das Mesoderm charakteristisch und es bildet das prominenteste Derivat, die Muskulatur. *Brachyury* (*Bra*), *even-skipped* (*eve*), *Mox* und *myosin II heavy chain* (*mhc*) sind Entwicklungsgene, die oft bei der Bildung des Mesoderms und der Muskeln beteiligt sind. Muscheln sind noch sehr unerforscht bzgl. Genexpressionen im Mesoderm und in Muskeln, sowie auch in der morphologischen Myogenese, jedoch sind sie eine wichtige Gruppe in der Evolutionsbiologie. Die oben genannten Entwicklungsgene und die Muskelentwicklung wurden bei der Quagga-Dreikantmuschel *Dreissena rostriformis* untersucht, um Fragen zum basalen larvalen Muskelbauplan der Autobranchia und um die Beteiligung dieser Gene an der Entwicklung des Mesoderms und der Muskulatur zu beantworten. Die Ergebnisse zeigen, dass alle vier Gene bei der Bildung des Mesoderms beteiligt sind und zusätzlich auch individuelle Expressionen aufweisen, sowie *Mox* und *mhc* in der Muskelentwicklung, *Bra* im Vorderdarm und *eve* im Schalenfeld. Vergleichende Analysen weisen darauf hin, dass *Mox* eine basale Expression in der Mesoderm- und Muskelbildung in den Bilateria hat, während *eve* und *Bra* eine konservierte Expression in der Mesoderm Entwicklung in den Nephrozoa hat. Die ersten F-Actin Domänen bilden sich in der *D. rostriformis* Trochophora Larve, sowie eine vorübergehende ventro-posterior Muskulatur mit einer unbekannten Funtion. In der Veliger Larve entwickeln sich vier Paare Velum Retraktoren, ein Velum-Muskelring, ein Paar Larval Retraktoren, Muskeln der Palliallinie, Mantle- und Fuß Retraktoren und ein zwei-teiliger anterior Adduktor. Der posterior Adduktor wurde nicht gefunden, dieser entwickelt sich wahrscheinlich vor oder nach der Metamorphose. Die derzeitigen Daten legen nahe, dass der basale larvale Muskelbauplan der autobranchen Muschel zu mindestens ein Velum-Muskelring, drei oder vier Paare Velum Retraktoren, ein oder zwei Paare Larval Retraktoren, zwei Paare Fußretraktoren einschließlich einer Fußmuskulatur, möglicherweise zwei Paare Mantel Retraktoren, Pallial Muskeln, einen anterioren und einen posterioren Adduktor enthält.